Therapeutic and diagnostic radiopharmaceuticals#

Attila Keresztes, Attila Borics, Csaba Tömböly*

Institute of Biochemistry, Biological Research Centre, Hungarian Academy of Sciences, Szeged, Hungary

ABSTRACT Medical application of ionizing radiation and radioactive isotopes were considered almost immediately after their discovery. The intense research interest in radioactivity, materials structure, subatomic particles and in the establishment of physical principles resulted in milestone inventions such as the radiotracer principle, particle accelerators, nuclear reactors and detectors sensitive enough to indicate different types of radiations even at very low intensities. This technical development together with advancements in pharmaceutical chemistry led to the establishment of nuclear medicine as a new discipline, and currently the prevalence of radiologic applications in today's medicine is obvious as tens of millions of nuclear medicine procedures are performed annually in more than 10,000 hospitals worldwide (World Nuclear Association 2014). In this review a brief historical outline of the most important discoveries and a summary of principles of radioactivity and radioactivity detection are given. Diagnostic and therapeutic application of radiopharmaceuticals, their production and their tissue-specific targeting methods are also discussed along with an introduction of state-of-the-art diagnostic modalities and a summary of further requirements and future perspectives.

KEY WORDS

nuclear medicine
radiopharmaceutical
diagnosis
therapy
radioactivity

Introduction

In 1895 Wilhelm Conrad Röntgen observed a unique electromagnetic radiation called X-rays. Later, in 1896 Henry Becquerel discovered natural radioactivity when he took the first image of a natural radioactive substance, zippeite. These basic observations initiated intense research concerning radioactivity, materials structure and subatomic particles. Today, tens of millions of nuclear medicine procedures are performed annually in more than 10,000 hospitals worldwide. Different types of radiations originated from radioactive decay are exploited by nuclear medicine to provide diagnostic information of the patients and to treat them. Indeed, nuclear medicine is one of the most sensitive methods today for obtaining information on physiological functions. The most common radioisotope for diagnosis is Tc-99m, with ca. 30 million applications per year, accounting for 80-90% of all nuclear medicine procedures (World Nuclear Association 2014). Radiotherapy is mainly used to treat different types of cancers by the specific destruction of malignant cells. Milestone discoveries of this rapid scientific and technological development are reviewed, and an overview of radiopharmaceutical applications is presented.

Submitted Febr 11, 2015; Accepted Oct 31, 2015
*Corresponding author. E-mail: tomboly@brc.hu
#This review is dedicated to the 70th birthday of Géza Tóth.

Development of nuclear medicine

Soon after the discovery of X-rays, their practical application in research and imaging became apparent. It was also observed that prolonged exposure to X-rays produced inflammation and tissue damage on the skin, which led to the application of irradiation in the treatment of skin diseases (Pusey 1900). After unambiguous X-ray therapeutic trials, Henry Coutard had developed a fractionated process that is the basis for current radiation therapy (Coutard 1937). Two years after Becquerel's discovery, Marie and Pierre Curie discovered two natural radioactive elements, Po-210 and Ra-226. The radiation of the latter one was immediately suggested to use in the therapy of skin lesion, and it was the first natural radioactive substance used in human medicine. The widespread medical applications of radioisotopes became feasible after the discovery of the radiotracer method by György Hevesy, the invention of the cyclotron by Ernest O. Lawrence and the discovery of artificial radioactivity by Irène Curie and Frédérick Joliot.

Hevesy recognized that the chemical properties of a compound and its isotopologues were identical, and consequently a radioactive atom might be used as a tracer of stable atoms of the same element in biological systems. A radiotracer is a compound containing one or more radioactive isotopes, and measuring the radioactivity of the tracer resulted in increased sensitivity and accuracy over existing methods.

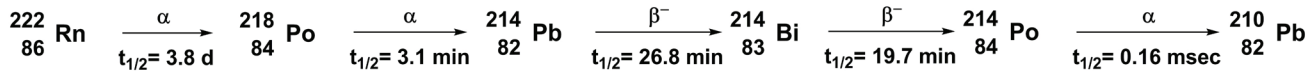

Figure 1. Segment of the decay chain used for the preparation of the first radiopharmaceutical, saline containing Pb-214 and Bi-214.

Hevesy described the radioactive tracer concept in 1913 and introduced it in life sciences (Hevesy 1923). In 1925, Hermann Blumgart performed the first human radiotracer experiment to study the cardiovascular system (Patton 2003). The diagnostic radiopharmaceutical prepared by Blumgart's procedure was a saline solution of Pb-214 and Bi-214 (Fig. 1). The Wilson cloud chamber modified by Shimizu (Shimizu 1921) and Yens (Blumgart et al. 1926) became the detector of choice, appropriate for dynamic detection in the circulating system. The optimized method required minimal cooperation of the patient and it was objective, noninvasive, and rapid enough to automatically detect the previously administered radioactive substance. The radioactive tracer was applied in a minute amount therefore it had no pharmacological effect. It highlighted the most important characteristic of a tracer, i.e. it can facilitate the study of components of a homeostatic system without disturbing their function.

Subatomic particles important for practical nuclear medicine (electron (Thomson 1897), proton (Rutherford 1919) and neutron (Chadwick 1932)) had also been discovered this period of time. Another important particle, the positron postulated in 1928 by Paul Dirac was first observed in 1932 by Carl D. Anderson (Anderson 1932).

Rutherford demonstrated the first artificial production of O-17 by bombarding N-14 with α particles, that was followed by the work of Frédérick Joliot and Irène Curie who achieved the first production of a radioactive isotope (Joliot et al. 1934). They investigated the bombardment of light elements with Po derived α particles, and they observed that in the case of Al the target remained active after the bombardment stopped. The radionuclide was identified as P-30 that decayed to Si-30. Before this groundbreaking discovery, Leó Szilárd filed two patents in Germany on a linear accelerator and on a cyclotron in 1928 and 1929, respectively, but they were never published. The development of the cyclotron, a device that makes it possible to produce larger amount of artificial radionuclides was first described by Earnest O. Lawrence and his students (Lawrence et al. 1932). By 1936 up to 200 radionuclides had been produced, and at present ca. 2500 isotopes are known among which there are up to 200 radioisotopes regularly used and mainly produced artificially.

The discovery of the cyclotron produced artificial radioactivity opened the way to the production of a variety of radioindicators useful for medical purposes. The phosphorous metabolism and cellular processes involving phosphorous containing molecules had pioneered by the work of Gy. Hevesy and O. Chiewitz. For their early experiments they used carbon disulfide to absorb neutrons emitted from a Ra-Be mixture, and then the aqueous extract containing P-32 was applied for life science studies (Chiewitz et al. 1935). Later P-32 was produced in larger quantities by Lawrence's cyclotron. Dynamics of sodium transport was investigated with Na-24 by J. G. Hamilton (Hamilton et al. 1937). I-128 was applied for the study of thyroid physiology (Hertz et al. 1938) and later for the diagnosis and treatment of Graves' disease. The adsorption of fluoride by enamel, dentine and bone was evidenced by using a F-18 tracer (Volker et al. 1940). The first radioactive iodine isotope, I-128 was discovered by E. Fermi in 1934, and four years later G. Seaborg discovered I-131. The latter one was immediately used for diagnostic purposes by J. G. Hamilton. In the 40s' numerous radioactive tracers were introduced in clinical medicine (Marshall 1990), followed by a continuous interdisciplinary work of physicists, chemists and physicians in order to develop detection instruments and radiopharmaceuticals which could be used to investigate (i) the underlying mechanisms of human diseases, (ii) the earliest manifestation of them in a noninvasive way, and (iii) their selective treatment. The detailed review of the evolution of nuclear medicine, especially the development of sophisticated detectors and computing algorithms in the second half of the 20th century is far beyond the scope of this review. Instead, the birth of the discipline is demonstrated and further important milestones are summarized in Table 1.

Principles of radioactivity

Radiopharmaceuticals are radioactive labelled substances containing one or more radionuclide(s) suitable for administration to humans. The chemical and physical properties of the radiopharmaceutical affect its localization in the body, while the radioactive decay properties determine the detection method and the diagnostic or therapeutic applicability. The emission of the diagnostic radionuclides is used to visualize the distribution of the labelled substance in the body, and that of the therapeutic radionuclides is used to deliver a high radiation dose to the target tissue.

The relative stability of nuclei can be compared via the binding energy per nucleon (E_B/A) (Fig. 2). Radioactive decay, a spontaneous nuclear transformation is a way for nuclides to achieve a more stable nuclear state. The time

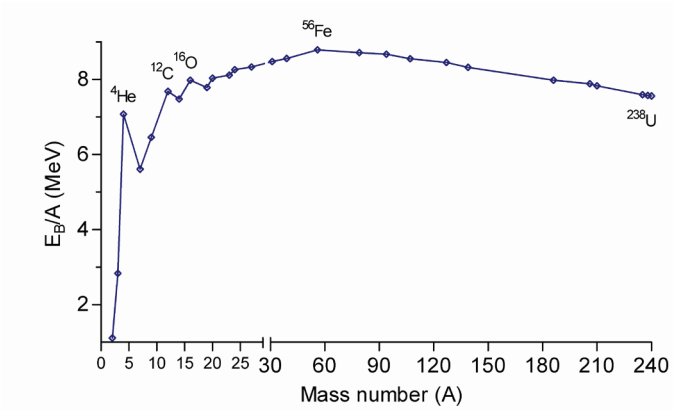

Figure 2. Binding energy per nucleon as a function of mass number.

dependence of radioactive decay is expressed in terms of the half-life ($t_{1/2}$), that varies in a wide range of time with the shortest measurable half-life of 10^{-18} s. Radioactive decay involves a transition from a definite quantum state of the original nuclide (parent) to a definite quantum state of the product nuclide (daughter). The energy difference between the two quantum levels corresponds to the decay energy that appears in the form of electromagnetic radiation and as the kinetic energy of the product particles (Choppin et al. 2002). The mode of radioactive decay depends on the particular radionuclide. Alpha decay is the emission of a He^{2+} (α particle), and with a few exceptions, only radionuclides heavier than lead and a few lanthanide elements decay by this way. An example is Ra-226 that produces Rn-222 and 4.78 MeV α particles. Soon after the discovery of radium, Ra-226 and its radioactive daughter Rn-222 were used in medicine. At present alpha radiation has no significant clinical usefulness. However, some α emitters are investigated for therapeutic applications, because α particles are the least penetrating type of radiation producing dense ionization and severe radiation damage within a tissue. Beta decay is the emission of either an electron or a positron, or the process of electron capture. Neutron-rich radionuclides undergo β^- decay resulting in the emission of high speed electrons (β^-) and antineutrinos with kinetic energies ranging up to the maximum value of the decay energy, E_{max}. These electrons travel several hundred times the distance of α particles in air and require a few millimeters of aluminum to absorb them. Positron decay occurs when the n/p ratio is too low for stability and a proton is transformed into a neutron followed by the ejection of a positron – antineutrino pair. Positrons are emitted with a continuous energy distribution but exist only for a very short period of time (ca. 1 μs), after which they loose most of their kinetic energy and combine with an electron. This annihilation results in two 511 keV photons emitted in opposite directions. Electron capture (EC) is another way for proton-rich nuclides to be stabilized. The nuclear composition changes similarly to that occurring in positron decay, but via a different mechanism: the nucleus captures an orbital electron, usually from the *K*-shell. Electrons from higher energy levels immediately fill the vacancy, and the excess energy of the orbital rearrangement(s) is emitted as a secondary radiation of a cascade of *characteristic X-ray* photons and Auger-electrons. EC and positron decay are competing processes, but if the parent proton-rich nuclide does not have at least 1.022 MeV of transition energy, a positron cannot be formed and only EC will occur. EC is advantageous for diagnostic applications because it does not produce particulate radiation that lowers the patient's effective dose. The following radionuclides used in nuclear medicine decay by EC: Cr-51, Co-57, Ga-67, In-111, I-123, I-125 and Tl-201.

The α and β decay may result in daughter nuclei in an excited state. When excited nuclei reach their ground state the transition energy is released either by electromagnetic radiation (γ radiation) or by internal conversion. The release

Table 1. Development of nuclear medicine(Ell 2014).

1895	X-rays (W.C. Röntgen)	1951	NaI crystals for positron detection (W. Sweet, G. Brownell)
1896	Radioactivity	1953	Cerebral blood flow with Kr-81m (N. Lassen)
1898	Po, Ra, Th (M. S. Curie)	1958	Anger gamma camera (H. O. Anger)
1923	Tracer principle (Gy. Hevesy	1959	Radioimmunoassay (R. S. Yalow, S. Berson)
1928	Gas filled counter (J. W. Geiger, W. Müller)	1962	Tc-99m generator (P. Harper, K. Lathrope)
1932	Cyclotron (E. O. Lawrence)	1962	SPET (D. Kuhl)
1934	I-128 (E. Fermi)	1973	Description of the CT scanner (G. H. Hounsfield)
1936	Tc-99m (E. G. Segre)	1973	First PET tomograph (M. Ter-Pogossian, M. Phelps)
1936	Therapeutic use of P-32 (J. H. Lawrence)	1978	[^{18}F]FDG (T. Ido)
1938	I-131 (G. Seaborg)	1997	FDA approves [^{18}F]FDG as radiopharmaceutical
1946	Thyroid cancer therapy (S. M. Seidlin, L. D. Marinelli)	1998	PET/CT prototype (D. Townsend, R. Nutt)
1949	Thyroid carcinoma therapy in Europe (C. Winkler, E. E. Pochin)	2000s	Revolution of hybrid tomographic imaging (PET/CT and SPECT/CT); end of 2D planar imaging
1951	Rectilinear scanner (B. Cassen)	2010s	Quantitative 3D imaging on hybrid devices, beginning of targeted therapies

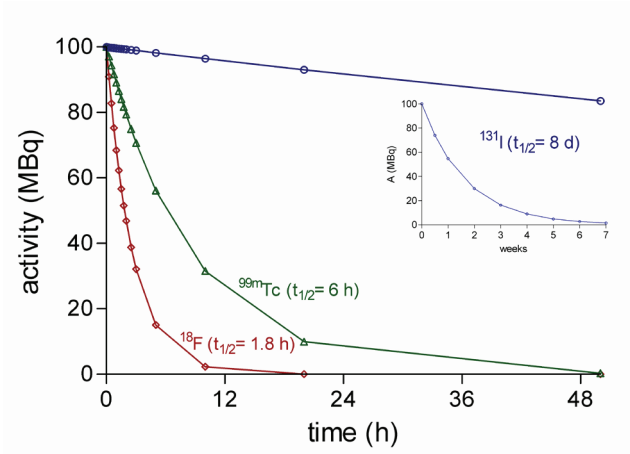

Figure 3. Decay of F-18, Tc-99m and I-131 over time.

of the nuclear energy excess by γ photon emission is known as isomeric transition (IT). The emission of photons from the excited nucleus occurs immediately after α or β decay (within 10^{-12} s), but in some cases the nucleus may remain in the excited state for a measurable period of time with a half-life in the range of 10^{-9} s to several months. These longer-lived metastable nuclei are called isomers and are designated with "m" after the mass number. Some metastable isomers have a half-life long enough for their chemical separation from the parent radionuclide. Such an example is Tc-99m, which is produced from Mo-99 in a technetium generator. Tc-99m undergoes de-excitation to its ground state isomer Tc-99 and during this process it emits a monoenergetic γ-ray of 140 keV:

$$^{99}_{42}\mathrm{Mo} \xrightarrow{\beta^-} {}^{99m}_{43}\mathrm{Tc} \xrightarrow{\mathrm{IT}} {}^{99}_{43}\mathrm{Tc} + \gamma$$

An additional process via an excited nucleus can achieve the ground state is internal conversion (IC). Because the wave function of an orbital electron may overlap that of the excited nucleus, the excitation energy can be directly transferred to an orbital electron without the involvement of a γ photon. If an electron absorbs the nuclear energy this way, it is ejected from the atom, and it is called conversion electron. Internal conversion and isomeric transition are competing processes, and the ratio between the number of conversion electrons and the number of γ photons is called conversion coefficient. For clinical imaging procedures the high photon abundance (IT) is desirable.

Description of the kinetics of the radioactive decay

The definition of radioactivity refers the decay rate of a radioactive substance:

$$-\frac{dN}{dt} = \lambda N$$

where N is the number of radionuclides, λ is the proportionality constant, called decay constant. If the original number of nuclei present at t= 0 s is N_0, then integration yields

$$N = N_0 e^{-\lambda t}$$

where N is the number of radioactive atoms remaining after time of decay, t. Since it is simpler to determine the disintegration rate than the number of radioactive atoms, the practical expression of the radioactive decay is

$$A = A_0 e^{-\lambda t} \quad \text{and} \quad \lambda = \frac{\ln 2}{t_{1/2}}$$

where A_0 is the original activity and A is the activity remaining after time of decay, t (Fig. 3). Originally, curie (Ci) was used as the basic unit of radioactivity, based on the disintegrations per second (dps) occurring in the quantity of radon gas in equilibrium with 1 g of radium. In 1950, the curie was redefined as 37 billion disintegrations per second (dps) regardless of its source or characteristics.

Detection of ionizing radiation

The detection of radiation and the measurement of its intensity and energy distribution are important for imaging, for the exact determination of the activity of the radiopharmaceuticals, for dosimetry of irradiations, and for radiation protection. Excitation and ionization are the basic processes forming the physical basis of radiation detection, where light resulting from fluorescent de-excitation, fluorescence photons or charged particles are collected and measured by photomultiplier tubes, scintillation detectors and either gas-filled or semiconductor devices, respectively. In nuclear medicine, gas ionization and scintillation detectors are used for most purposes.

Gas ionization detectors

Gas-filled ionization detectors are ion chambers by principle. Ion pairs formed from the filling gas atoms or molecules by the passage of the ionizing radiation are separated in an electrical field, and electrons collected on the anode produce a pulse. Gas ionization detectors are characterized by the effects created at different field strength between the electrodes, because the pulse size depends both on the field strength and on the type of radiation (Fig. 4). In the ioniza-

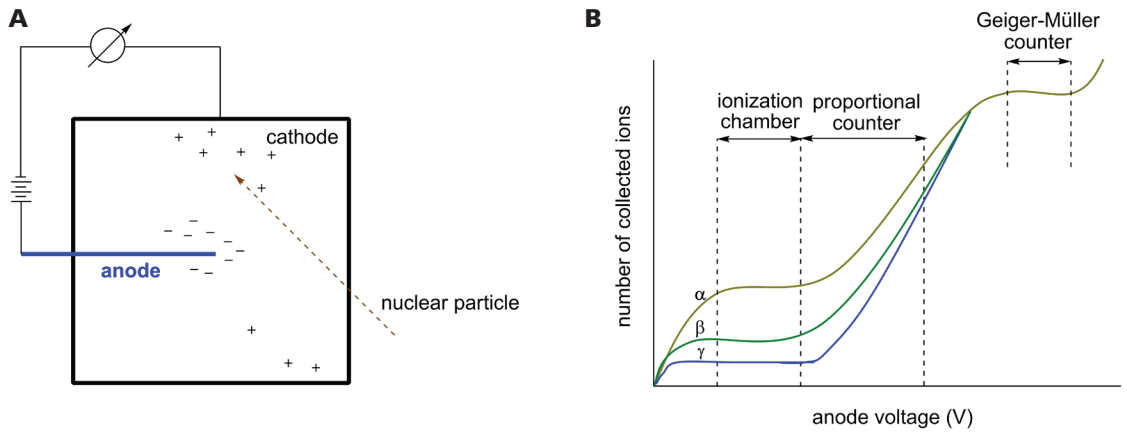

Figure 4. (A) Schematic representation of a gas-filled ionization detector. Electrons and cations are produced by the ionization of the filling gas exposed to ionizing radiation. Electrons collected by the anode produce a current which depends on the type and energy of the particle and also on the applied electric field. (B) The relationship between the pulse size produced and the potential applied across the electrodes.

tion region the rapid ions are not recombined and a saturation region is reached where all the primary electrons are collected. Detectors working under these circumstances are called ionization chambers that are used in dosimetry and in determining high levels of radioactivity (*e.g.*, multicurie Tc-99m generators, high-activity I-131 shipments). At higher field strength, electrons from the primary ionization receive sufficient acceleration to produce additional ionization. This multiplication process results in electrical pulses linearly proportional to the energy deposited in the detector by the passage of the radiation, and also different types of radiation can still be discriminated. Proportional counters operate in this region. Beyond the proportional region, the gas multiplication becomes very high, and the size of the electrical pulses is independent of the initial ionization, and also independent of the type and energy of the radiation. Geiger-Müller (GM) counters which operate in this region have high sensitivity to different types of radiation. GM detectors are limited to use for measuring low levels of radiation, but are frequently used in nuclear pharmacy for monitoring personnel and radioactive contamination in work areas.

Particles are easily detected by ionization chambers as they produce great number of ions along a short path. The ionization and excitation effects of the β^- particles are weaker than that of the α particles, and thus, their measurement requires amplification. It is achieved by proportional or GM counters, or by scintillation counting. Gamma rays produce very low density ionization in gases, therefore they are counted by solid scintillation counting or with semiconductor detectors.

Scintillation detectors

In scintillation counting, fluorescence photons are detected which are emitted during de-excitation of molecules excited by ionizing radiation. Both liquid and solid scintillation methods are applied in nuclear medicine and nuclear pharmacy. In liquid scintillation measurements the radioactive sample is dispersed in a solution of an organic scintillator. It provides highly efficient detection of β particles, but also used for the quantitative analysis of α, weak γ, X-ray and Auger e^- emitters. The molecular interactions leading to photons are represented on Figure 5 including processes that decrease the counting efficiency in liquid scintillation counting.

Solid scintillation detectors typically use inorganic crystalline materials such as NaI(Tl), CsI(Tl) and $Bi_4Ge_3O_{12}$. Tl-activated NaI crystals (NaI(Tl)) are the most commonly used solid scintillators for γ or X-ray photon measurements. The principal mechanisms of interaction between γ or X-ray photons and matter are photoelectric effect, Compton-effect and pair production, all of which provide electron – hole pairs in the crystal. These electrons and holes are trapped by Tl^+ ions followed by radiative recombination of trapped electrons with free holes to form excited $[Tl^+]^*$. Light emission takes place upon the deactivation of $[Tl^+]^*$, and these light photons are detected by a PMT. NaI(Tl) is used for the detection of the 140 keV γ photons emitted by Tc-99m, the most widely used SPECT nuclide.

The principal image-forming detectors in nuclear medicine are SPECT cameras and PET scanners. Hybrid systems combine these detectors with computed tomography (CT). The practical application of the detection of single photon emitting radionuclides has been developed after the introduction of the NaI(Tl) scintillation camera by Hal Anger (Anger 1952). It consists of a large-area continuous NaI(Tl) crystal and an array of PMTs in combination with an absorptive collimator. This detector design provides spatial information on individual photon interactions and allows the creation of

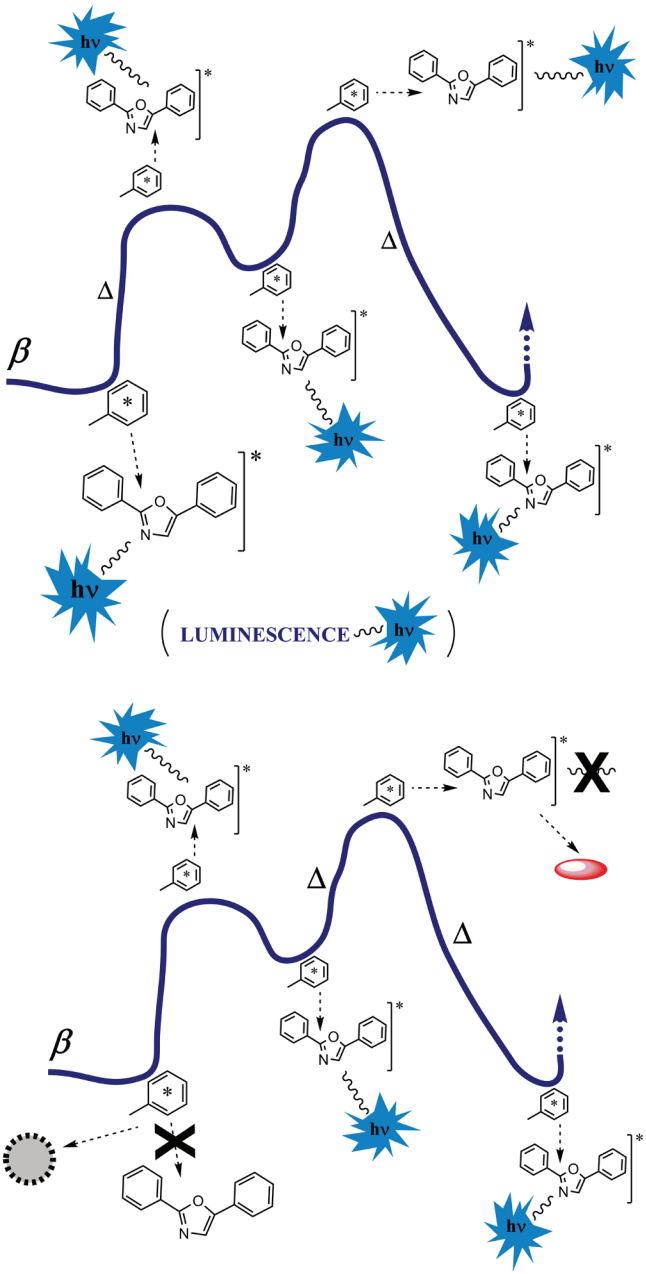

Figure 5. (A) Liquid scintillation in toluene solution in the presence of the scintillator 2,5-diphenyl-1,3-oxazole (POP). (B) Points of interference caused by chemical, photon and color quench are indicated.

two-dimensional images of the radiopharmaceutical distribution. Planar imaging of this type is called scintigraphy, and a typical example of this technique is bone scintigraphy. Such two-dimensional images recorded at multiple angles are reconstructed into a three-dimensional radiopharmaceutical distribution image in SPECT.

Positrons interact with matter similarly to electrons, but as the kinetic energy of the positron decreases, the probability of

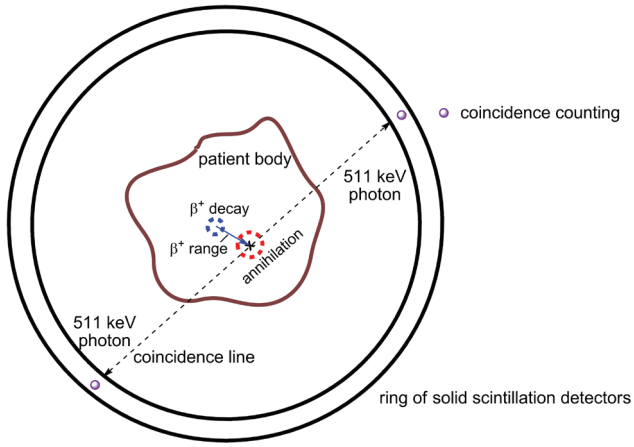

Figure 6. Detection of annihilation photons in PET.

direct interaction with an electron increases in which both particles are annihilated. The energy of the two electron masses is converted into two photons with equal energy. The co-linear property of these photons allows them to be detected simultaneously by opposing detectors in coincidence (Fig. 6). These coincidence lines are processed by an image reconstruction algorithm to generate cross-sectional images of the activity distribution of the radiopharmaceutical. Because coincidence detection is used in PET, the application of collimators is not required, that in turn increases the detection sensitivity by a factor of 10 – 100 over SPECT cameras. Modern scanners have a resolution of 4–6 mm that is almost the physically possible maximal resolution. Common scintillators in modern PET scanners are BGO ($Bi_4Ge_3O_{12}$), LSO ($Lu_2SiO_5(Ce)$) and GSO ($Gd_2SiO_5(Ce)$) with high light yield and fast responses during the detection of annihilation photons.

Production of radiopharmaceuticals

All radionuclides used in current nuclear medicine are produced artificially either in a nuclear reactor or in a particle accelerator by forcibly altering the nuclear structure of a stable target material. Currently ca. 80% of the medical radioisotopes are produced by neutron activation in a nuclear reactor, and the remaining isotopes are made by particle accelerators, mainly with cyclotrons. This ratio will be presumably changed, as cyclotrons offer many advantages over a nuclear reactor: (i) the volume of radioactive waste produced by cyclotrons is far less and less hazardous; (ii) the production is decentralized, *i.e.* the location of cyclotrons are hospital-based, resulting in more secured delivery of pharmaceuticals to patients and excluding the risk of transport accidents; (iii) there is no need for controlled chain reactions, therefore

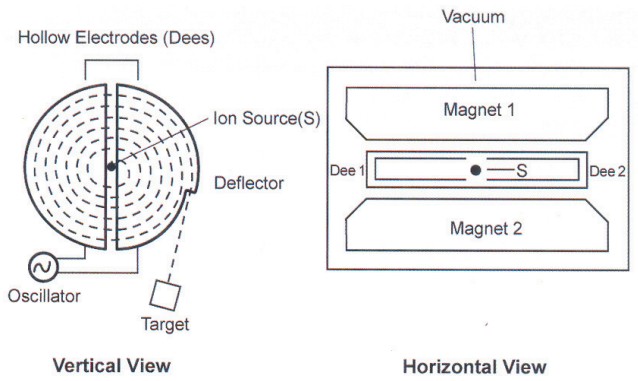

Figure 7. Schematic diagram of a cyclotron.(Kowalsky et al. 2011) The trajectory of the accelerated particle is represented by a dashed spiral. Repeated application of accelerating voltages to ions by the hollow electrodes (dees) accelerates ions to high velocities.

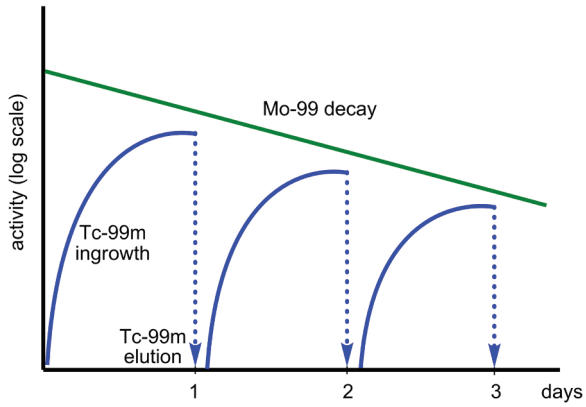

Figure 8. Relative activity of Mo-99 and Tc-99m in the generator over time. Maximum buildup of Tc-99m activity is reached in ca 23 h followed by elution.

there are no risk of nuclear-power accidents and nuclear proliferation.

Nuclear reactors used for isotope production have special ports where target materials can be introduced into the neutron flux resulting in neutron activation of stable nuclides into radioactive isotopes. The (n,γ) reaction is a general nuclear reaction resulting in an isotope of the target nuclide (e.g. ^{152}Sm(n,)^{153}Sm and ^{50}Cr(n,)^{51}Cr). If the product nuclide has a short half-life and decays to a longer-lived radionuclide, that can be isolated (e.g. ^{130}Te(n,)^{131}Te ($^{-}$)→ ^{131}I ($t_{1/2}$(Te-131)= 25 min, while $t_{1/2}$(I-131)= 8 d). Fast neutrons can also be captured by target nuclei in an (n,p) reaction (^{32}S(n,p)^{32}P). This reaction is advantageous because the product nuclide can be separated from the target resulting in high specific activity products. Many radionuclides are isolated among the fission products of U-235 including Xe-133, I-131 and Mo-99.

In a cyclotron, charged particles are accelerated along a spiral path by a radiofrequency electric field, and the trajectory is held fixed by a static magnetic field (Fig. 7). For nuclear medicine purposes two types of cyclotrons are used: positive ion instruments that accelerate protons and negative ion instruments that accelerate positronium ions (H^-). Modern cyclotrons are positronium accelerators where the accelerated H^- ions pass through a carbon foil, which strips away electrons and the resulting protons are immediately used to bombard the target (*e.g.* ^{111}Cd(p,n)^{111}In and ^{18}O(p,n)^{18}F). Radionuclides produced this way are not isotopes of the target nuclide, therefore they can be separated by chemical methods and high specific activity products are obtained. If the product nuclide has a short half-life, *e.g.* in the case of PET agents, an on-site cyclotron is required.

In radiation therapy and diagnostic medicine it is preferred to use short-lived radionuclides, because it decreases the effective dose of the patients during imaging, and also eliminates the problem of residual radioactive waste disposal.

A general solution is that a long-lived parent nuclide is stored and the short-lived daughter is isolated in the hospital as required for the nuclear medicine procedure. These systems are called radioisotope generators. A few appropriate nuclide pairs are summarized in Table 2. The most frequently used generator is based on the transient equilibrium of Mo-99 and Tc-99m (Fig. 8). The daughter nuclide Tc-99m is eluted by isotonic saline from an alumina column where the daughter Mo-99 is adsorbed. The resulting [^{99m}Tc]$NaTcO_4$ solution is used for the preparation of Tc-99m radiopharmaceuticals that generally includes reduction of Tc(VII) with Sn(II) followed by complexation with different chelators.

Dosimetry

Radiation protection uses the concept of effective dose that refers to the dose averaged over the entire body, and it takes into account the relative biological hazard of different types of radiation and also the relative sensitivity of different areas of the body. It allows for the quantification of health risk and also for the comparison of irradiation sources like natural

Table 2. Common radionuclide pairs applied in generator systems.

Parent ($t_{1/2}$)	Decay	Daughter ($t_{1/2}$)	Decay	Application
Ge-68 (270 d)	EC	Ga-68 (68 min)	β^+ (1.9 MeV), EC	PET
Rb-81 (4.5 h)	EC	Kr-81m (13 s)	IT (191 keV γ)	imaging
Sr-82 (25 d)	EC	Rb-82 (75 s)	β^+ (3.18 MeV)	PET
Sr-90 (28.8 y)	β^-	Y-90 (64 h)	β^- (2.28 MeV)	therapy
Mo-99 (66 h)	β^-	Tc-99m (6 h)	IT (140 keV γ)	imaging
Sn-113 (115 d)	EC	In-113m (1.7 h)	IT (393 keV γ)	imaging

Table 3. Average effective dose values of different procedures, activities.

Source of radiation exposure	Effective dose
Radiation sickness	> 1 Sv immediately
Coronary angiography	16 mSv
[^{67}Ga]Ga-citrate (4 mCi) body scan	15 mSv
[^{18}F]FDG (20 mCi) brain PET scan	14 mSv
Mammography (X-ray)	4 mSv
Natural background radiation (worldwide average)	2.4 mSv/y
Head CT	2 mSv
[^{123}I]NaI (0.25 mCi) thyroid scan	1.9 mSv
[^{111}In]pentetreotide (6 mCi) body scan	1.2 mSv
Dose limit for the general public	1 mSv/y
[^{133}Xe]Xe (20 mCi) lung ventillation	0.5 mSv
Chest X-ray	0.1 mSv

background radiation or nuclear medicine procedures (Table 3). The effective dose is the sum of the equivalent doses in all organs and tissues weighted for the specific sensitivity of the organs and tissues. The equivalent dose is the radiation dose absorbed by an organ or tissue weighted for the type of radiation. Thus, the effective dose provides one number that reflects the whole body risk from non-uniform radiation exposure. The unit of the effective dose is sievert (Sv). The upper limit of the administration of a radiopharmaceutical is determined by these dose values, and the health risk of patients is also calculated from equivalent dose to individual organs and effective dose to the whole body values.

A major problem in radionuclide therapy is currently that there is no accepted standard method for calculating the absorbed dose from internal radionuclides. In an attempt to standardize dosimetry, the European Association of Nuclear Medicine (EANM) has recently issued a guidance document on 'Good Practice of Dosimetry Reporting', which makes recommendations for optimal internal dosimetry (Eberlein et al. 2011; Lassmann et al. 2011). At present, dosimetry in radionuclide therapy relies on the medical internal radiation dose (MIRD) formulation, which is based on the calculation of the average tumor-absorbed dose at a macroscopic level. This calculated dose assumes a homogenous distribution of radionuclides in organs, whereas spatial heterogeneity of internalized radionuclides exists at tissue and cellular levels (Brans et al. 2007). Heterogenic distribution of radionuclides leads to unevenly absorbed dose that may result in unsuccessful radiotherapy.

The principles of tumor dosimetry for targeted therapy with internally administered radiopharmaceuticals are similar to those for external-beam radiation therapy (EBRT). The maximum absorbed radiation doses to critical organs are mostly related to experiences with EBRT. Dosimetry enables the conversion of the total number of radionuclide transformations in a particular source tissue to absorbed dose in a target tissue. Such conversion requires information on emission properties of the radionuclide as well as source-target tissue anatomy and composition. Monitoring toxicity allows physicians to reduce doses of repeatedly given radiopharmaceuticals though, "underdosing", which may lead to lower efficacy, remains an important concern. The other important aspect is the prediction of tumor response and toxicity following radionuclide administration.

Dose quantities such as equivalent uniform biologically effective dose (EUBED), therefore, may be valuable complements to EBRT doses in targeted radiotherapy. With the current advances in radiobiological modeling, it is conceivable that EUBED and tumor control probability calculations could routinely make part of patient-specific treatments in the future (Chianelli et al. 2011).

Radionuclide delivery systems, significance of formulation

In spite of the wide variety of radiolabelled agents that have been developed and applied clinically for the diagnosis and treatment of malignant conditions over the past decades, the number of diagnostic and therapeutic radiopharmaceuticals that has received approval for routine clinical use is very low (Dash et al. 2013). Since the design of selective radiotherapeutic agents encounters multiple difficulties such as specific *in vivo* targeting of the tumor cells, clearance of radioactivity from non-target tissues and decay properties of the radionuclide, drug formulation and other derivatization strategies had to be developed (Aerts et al. 2014; Volkert et al. 1999).

Peptide and protein-based carriers

Chelate formation and/or subsequent chemo- or bioconjugation to transport molecules (peptides or proteins) is one of the most widely used formulation (e.g. Ga-68, Tc-99m, Sr-89, Y-90, In-111, Lu-177, At-211, Ac-225 or Ra-223 chelated by NTMP, EDTMP, DTPMP, DOTMP, NTA, EDTA, DTPA, DOTA) that serves for targeted delivery and enhanced specific radioisotope accumulation (Fig. 9) (Volkert et al. 1999). Beyond preventing isotope exchange, these chelators enable easy coupling of radionuclides to carriers and the resulting radiopharmaceuticals display improved pharmacodynamic and farmacokinetic characteristics (Attard et al. 1995; Jánoki et al. 1992; Volkert et al. 1991).

A series of radiolabelled peptides have been designed and optimized for tumor-targeted peptide receptor radionuclide therapy using the aforementioned complexes (Dong et al. 2014; Fani et al. 2012a; Okarvi 2008). Pre-clinical and clinical applications of this strategy have shown encouraging results on tumor response, overall survival, and quality of life

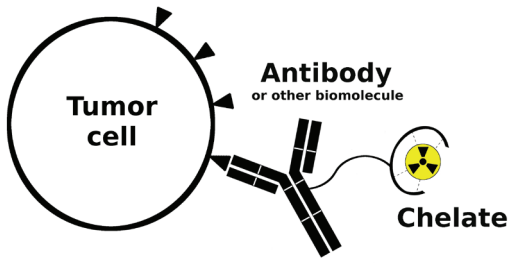

Figure 9. A representative model of a radionuclide-chelate-carrier conjugate. Depending on the radionuclide used, the complex can be applied for molecular imaging (PET) or radioimmunotherapy (RIT). The construct contains a chelated radionuclide which is bound to a carrier (peptide or antibody) that recognizes tumor antigens on the surface of cancer cells.

in patients with different tumors. Y-90-DOTA-TOC and Lu-177 or Ga-68-DOTA-TATE radionuclide-chelate conjugates are the most common radiopharmaceuticals in detecting and targeting endocrine and neuroendocrine tumors (Bodei et al. 2004; Bodei et al. 2013; Forrer et al. 2006; Haug et al. 2010). The Y-90, In-111 or I-131 labelled antibody- or octreotide-based radiopharmaceuticals directed against the glycosylated, cell-surface phosphoprotein CD20 or somatostatin receptors, and that are used in the treatment of non-Hodgkin lymphoma and different neuroendocrine tumors, are further examples of this strategy (Kaltsas et al. 2005; Paganelli et al. 2002). In addition to the somatostatin analogs, other radiolabelled peptides have also been developed for tumor cell overexpressing receptors such as integrin V 3, gastrin-releasing peptide receptor (GRPR), melanocortin-1 receptor (MC1-R), cholecystokinin (CCK) receptor, and glucagon-like peptide-1 receptor (GLP-1R) (Dong et al. 2014; Fani et al. 2012a, 2012b).

Carrier-bound radioisotopes which bind cytoplasmic proteins or nuclei of cancer cells, represent another diagnostic and therapeutic application. Cell-penetrating peptides are examples of such carriers that are capable of carrying radioisotopes into cells (Kersemans et al. 2008; van Duijnhoven et al. 2011). These peptides possess a short Arg-rich sequence that facilitates internalization of the radioisotope-peptide conjugate. Other members, such as the viral nuclear TAT protein and nuclear localizing peptides are able to deliver radionuclides or cell cycle control molecules into the nucleus where they can exert DNA damaging effects (Cornelissen et al. 2012a; Mishra et al. 2011). This latter approach proved to be advantageous for radionuclides that emit particles of extremely short path length (Auger electrons) and when incorporated or localized in close proximity to DNA (Hu et al. 2007).

Radionuclide conjugated circulating monoclonal antibodies, antibody fragments are routinely used in radioimmunotherapy, diagnosis and tumor pre-sensitization strategies. Antibodies can recognize specific receptors and deliver high doses of radiation into tumor cells. These agents are directly radio-iodinated or chelated with macrocyclic chelators (*i.e.* DOTA) carrying the radionuclide that is often a β emitter such as Y-90 or I-131 (Forero et al. 2005; Reardon et al. 2002).

Nano-assemblies

Recent advances in nanotechnology has prompted the use of nanoparticles as carriers for radiotherapeutics. Inorganic multivalent nanoparticles that dispose of optical (*e.g.* gold nanoparticles, carbon nanotubes) or magnetic (*e.g.* iron oxide) properties, can be exploited for thermal-ablation therapy of malignant tumors or molecular imaging. As a result of their multivalency, other types of radiolabelled nanoparticles, composed of self-organizing materials have proven to be promising tools as multimodal imaging agents in the diagnosis and therapy of malignant processes (Ferro-Flores et al. 2014; Xing et al. 2014).

Radiolabelled nanoparticles offer the potential for delivery of a large payload to tumors since nanoparticles tend to passively accumulate in tumors with disorganised vasculature (Goins 2008; Torchilin 2011). Liposomes loaded with Ac-225 labelled trastuzumab have been shown to bind and internalized into HER2/neu overexpressing cells (Sofou et al. 2007). Similarly, folate receptor targeting poly(lactate-co-glycolate) copolymer nanoparticles encapsulating docetaxel and Y-90 radionuclide have been developed for the therapy of peritoneal metastases in ovarian cancer (Werner et al. 2011). Other nanoparticle formulations such as dendrimers, carbon nanotubes, silica nanoparticles capable of directing therapeutic radionuclides into tumor cells have also been investigated (Di Pasqua et al. 2013; Hong et al. 2010; Ting et al. 2009). Carbon nanotubes covalently linked to anti-endothelial-cadherin antibody loaded with Zr-89 for PET imaging and with Ac-225 for a particle therapy of a murine xenograft model of human colon carcinoma are further examples of this approach (Ruggiero et al. 2010). Currently, the development and clinical trial of dual function "theranostic" nanoparticles for both imaging and radiotherapy are in progress (Xing et al. 2014).

Radiolabelled microspheres have been used for delivering localized radiation dose to tumors for different organs following intraarterial administration (Häfeli 2001; Muller et al. 1951). These microspheres have a size of ≥ 10-15 μm which is enough to lodge in the arterioles or capillaries of solid tumors having well-organized vasculature. Several types of particles and microspheres (Y-90 labelled-Y_2O_3 particles, Y-90 ceramic microspheres, Y-90 resin microspheres, and Y-90 glass microspheres) have been used with promising results, especially against liver malignancies (Deleporte et al. 2010; Harbert et al. 1987).

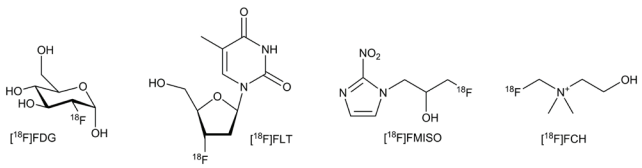

Figure 10. Structure of F-18 radiopharmaceuticals.

Diagnostic radiopharmaceuticals

Imaging procedures are non-invasive investigations that provide diagnostic information by measuring the distribution of radioactivity in the human body under normal and pathological conditions. In nuclear medicine imaging the position of the radiation source within the body is detected, that is the fundamental difference from other imaging techniques, such as X-rays. In dynamic studies the rate of accumulation and clearance of the radiopharmaceutical are determined, while static imaging provide morphological information by detecting the radioactivity accumulated in the organ of interest. Detection and measurement of organ radioactivity is generally performed with a gamma camera. In current clinical practice the most common imaging techniques (excluding X-rays) are computed tomography (CT), magnetic resonance imaging (MRI), ultrasound, planar scintigraphy, and single photon emission computed tomography (SPECT), positron emission tomography (PET) and magnetic resonance spectroscopy (MRS). Tomographic imaging (SPECT and PET) delineate high-resolution structural and functional information by constructing computer-generated transverse, sagittal and coronal slice images of an organ. Planar scintigraphy, CT, SPECT and PET make use of ionizing radiation, and except for CT, these imaging methods require the administration of medical radioisotopes. These tracers are generally short-lived radionuclides bound to chemical compounds which permit specific physiological processes to be investigated.

Positron emission tomography (PET) and its diagnostic use

With the recent advances in radiotracers and imaging techniques PET has become one of the most powerful and revolutionary methods in medical sciences and diagnosis. It is a high-spatial-resolution, sensitive and functional nuclear imaging technique that allows repeated *in vivo* non-invasive assessment and quantification of specific biochemical and physiological processes at molecular level (Clifford 2014; Mitterhauser et al. 2014). The principle of PET is based on the three-dimensional mapping and quantification of the distribution of a radiotracer that is labelled with a positron-emitting radioisotope (C-11, F-18, N-13, O-15, Cu-64, Y-86, Br-76, Ga-68, Rb-82 or I-124). It is usually introduced by injection and accumulates in the target tissue. As it decays it emits a positron, which combines with a nearby orbital electron resulting in the simultaneous emission of two gamma photons with the same kinetic energy (*i. e.* with the same tissue penetration property) in opposite directions. These photons are detected by the PET camera ring and the reconstructed images provide functional information on the target organ or tissue, on their metabolic activity, still before the anatomical signs of the disease are observed.

One of the most often used radionuclides for imaging purposes is F-18 (Fig. 10). This may be due to its favorable physical ($t_{1/2}$= 109.8 min) and nuclear characteristics, and also, to the successful use of [^{18}F]fuoro-2-deoxy-D-glucose ([^{18}F]FDG) in diagnostic and clinical oncology (Cai et al. 2008; Dolle 2013; Miller et al. 2008). Metabolic glucose imaging has been the primary use of [^{18}F]FDG. This imaging modality has been used for the measure of metabolic activity, mostly in neurodegenerative and cardiovascular diseases (Nasrallah et al. 2013; Palumbo et al. 2014). [^{18}F]FDG is physiologically and homogeneously distributed thorough cerebral and peripheral tissues, and tumors are visualized as lesions with higher or lower radiopharmaceutical uptake, compared with normal parenchyma (Fig. 11) (Palumbo 2008).

In recent years, other radiopharmaceuticals more tumor-selective than [^{18}F]FDG have been developed. F-18 labelled choline analogues have been synthesized for the diagnosis of brain and prostrate cancers (Giovacchini et al. 2010; Treglia et al. 2012). Other F-18 labelled radiopharmaceuticals are *O*-(2-fluoroethyl)-L-tyrosine ([^{18}F]FET) and 3,4-dihydroxy-6-fluoro-L-phenylalanine ([^{18}F]DOPA) (Chen 2007; Grosu et al. 2011). They have a brain tumor uptake similar to that of the [^{11}C]Met (Chen 2007), with the advantage of a longer half-life, with respect to C-11 labelled compounds. Kinetic studies have shown that Met has a significantly higher uptake in all cells examined, with respect to FET. Furthermore, inflammatory cells preferentially incorporate Met than tumor cells, while significantly higher FET uptake was assessed in tumor cells. [^{18}F]DOPA has been used to image brain tumors due to high tumor uptake with respect to normal brain parenchyma (Pafundi et al. 2013). [^{18}F]DOPA can be considered useful in investigating brain metastases for the ability to cross the blood brain barrier, the low distribution in normal gray and white matter and the high tumor to normal tissue ratios.

A further F-18 labelled radiopharmaceutical is 3'-deoxy-3'-fluorothymidine ([^{18}F]FLT) that is used to image cell proliferation *in vivo* (Ullrich et al. 2008). [^{18}F]FLT is phosphorilated by thymidine kinase 1 (TK1) and as a result it accumulates in the cell. Tumor cells have a higher rate of proliferation, therefore they have an elevated activity of TK1 compared to normal tissue, which leads to a higher rate of accumulation of [^{18}F]FLT, which facilitates their detection using PET.

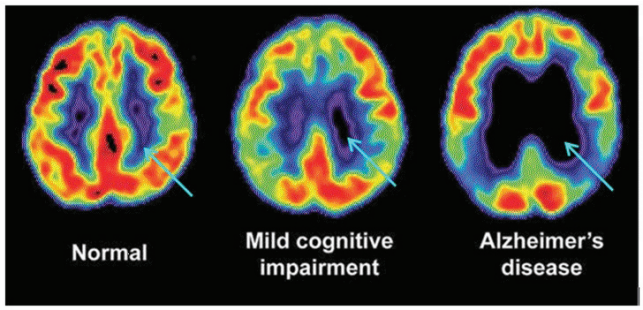

Figure 11. [^{18}F]FDG PET showing metabolic differences in normal and pathological human brains. Orange areas show high glucose uptake and increased metabolism, while spreading dark spots indicate progressive neurodegeneration and cell death.

C-11 ($t_{1/2}$= 20.38 min) is another PET radionuclide, though routine work with this radionuclide requires a cyclotron on site. Despite this disadvantage, the interest for C-11 is more intense since C-11 labelling of compounds can give radiotracers with unchanged pharmacokinetics and pharmacodynamics (Miller et al. 2008; Roeda et al. 2007). In comparison with F-18, C-11 labelled radiotracers offer exploration of *in vivo* metabolic pathways, and are often used with F-18 labelled compounds in parallel. Chemically, C-11 methylation is by far the most versatile method for the introduction of C-11 into radiopharmaceuticals, and radiolabelled reagents such as methyl-iodide ([^{11}C]CH_3I), methyl-triflate ([^{11}C]$CH_3O(SO_2)CF_3$) and phosgene ([^{11}C]$COCl_2$ are most widely applied for this strategy (Nagren et al. 1995; Wuest 2007).

Single photon emission computer tomography (SPECT) and its diagnostic use

Although, positron-emitting radiopharmaceuticals represent the ideal *in vivo* biomarkers for tumor and metastasis imaging, gamma-emitting radiopharmaceuticals visualized by SPECT, are useful, since the production of the radiopharmaceutical does not require an on-site cyclotron. However, the resolution is lower as compared to PET. Organ malfunction can be indicated if the radionuclide is either partially taken up by an organ, or taken up in excess over a period of time (Palumbo et al. 2014; Sogbein et al. 2014). The most frequently used gamma-emitter is Tc-99m, and a large number of Tc-99m based radiotracers have been developed including sestamibi (Higley et al. 1993; Jones et al. 1984; Wackers et al. 1989), tetrofosmin (Platts et al. 1995), and teboroxime (Johnson et al. 1990). Sestamibi and tetrofosmin have seen widespread clinical use, because they meet the requirements for myocardial perfusion, and a straightforward radiochemical synthesis and purification is available for them (Sogbein et al. 2014). In addition, [^{99m}Tc]tetrofosmin has been shown to accumulate intracellularly in actively proliferating cells, and thus, widely used as a neuro-oncological radiotracer in brain tumors (Palumbo et al. 2014).

Recently, more selective and potent Tc-99m complexes have been introduced and tested in therapy. These new agents contain cationic Tc-99m nitrido complexes, coordinating either bidentate dithiocarbamate or tridentate bisphosphine-type chelates (Bolzati et al. 2002; Boschi et al. 2002; Boschi et al. 2003). These derivatives demonstrate high cardiac uptake, long-time retention and nearly complete elimination from hepatocytes of Sprague-Dawley rats. Their heart/liver ratios were found to be higher than that of the [^{99m}Tc]sestamibi.

A gamma-emitting radiopharmaceutical, [^{123}I]-iodo-α-methyl tryrosine, ([^{123}I]IMT) was defined as a SPECT tracer. [^{123}I]IMT shares similar properties with other positron-emitting amino acid tracers, and is supposed to be incorporated via a stereo-selective active transport mechanism into neuronal cells (Palumbo 2008). Its uptake demonstrates relationship with cell proliferation and thus being applicable for the detection of malignancies of the central nervous system. Another I-123 labelled radiopharmaceutical is [^{123}I]meta-iodobenzylguanidine ([^{123}I]mIBG), that is the most extensively studied norepinephrine analogue for SPECT imaging of heart failure and central nervous system diseases. It shares similarities with norepinephrine with respect of storage, reuptake and release in presynaptic sympathetic nerve terminal (Bristow et al. 1982; Jacobson et al. 2010; Verberne et al. 2008). Its I-131 labelled counterpart has long been used as a radiopharmaceutical for the treatment of neuroblastomas.

Recent studies have shown that the PET radiotracer [^{18}F]FDG may be a more promising tool for the imaging of inflammation than the [^{99m}Tc]annexin-V conjugate, originally developed for the investigation of apoptosis with SPECT (Laufer et al. 2009). [^{18}F]FDG is an inflammatory marker which accumulates in actively recruited and metabolically active leukocytes, specifically macrophages. This property can be specifically exploited for the imaging of the inflammatory processes of the coronaries (Rogers et al. 2010; Rudd et al. 2002).

Multimodality imaging

Noninvasive multimodality imaging is a combination of different modalities such as nuclear medicine and radiology that offers revolutionary opportunities in clinical practice. In synchronous multimodality imaging, which is by far the most effective imaging technique, morphological and functional information are merged and processed in time and space. Ideally, any multimodal imaging approach should provide a more exact localization, extent and metabolic activity of the target tissue, facilitating faster and more accurate diagnosis. Data interpretation is based on tissue blood flow or morpho-

logical and functional changes that indicate the presence of any disease (Marti-Bonmati et al. 2010).

There are many multimodal technologies, but the most commonly used are SPECT-CT, PET-CT, PET-MRI and functional MRI combined with near infrared spectroscopy. Although SPECT-CT and PET-CT are becoming standard practice, MRI imaging has advantages over PET, SPECT and CT. It provides better soft-tissue contrast and multi-dimensional functional, structural and morphological information (Marti-Bonmati et al. 2010). The fMRI-NIRS modality is generally used for measuring tissue oxygenation/deoxygenation (ischemic conditions). Recently, combination of functional MRI and magnetoencephalography (MEG) or two-dimensional electroencephalography (EEG), have been used successfully for the measurement of neural electrical activity. This approach may have significance in the research and diagnosis of neurodegenerative diseases (Czisch et al. 2004; Martinez-Montes et al. 2004).

Therapeutic radiopharmaceuticals, targeted tumor therapy

Therapeutic procedures are either curative or palliative and essentially rely on the absorption of radiation to destroy diseased tissue. Rapidly dividing cells are particularly sensitive to damage by irradiation. For this reason, some cancerous growths can be controlled or eliminated by irradiating the area containing the growth. External irradiation can be carried out using a γ beam from a Co-60 source, or using high-energy X-rays produced by linear accelerators. Treating leukaemia may involve a bone marrow transplant, when the defective bone marrow is killed off with a massive dose of irradiation followed by implanting healthy bone marrow from a donor. Internal radiotherapy is achieved by administering or planting a source of ionizing radiation, usually a γ or β emitter, in the target area. Ir-192 implants are used especially in the treatment of head and breast cancers. They are produced in wire form and are introduced through a catheter to the target area, and after administering the appropriate dose, the implant wires are removed. This brachytherapy (short-range) procedure gives less overall radiation to the body, and is more localized to the target tumor.

α particle emitting radiopharmaceuticals and their therapeutic use

The use of α particle emitting isotopes, such as Bi-213, At-211, Ac-225, Th-227 and Ra-223 for targeted radiopharmaceutical therapy has been the subject of intense research over the past decade. Due to their short pathlength, α particles can only traverse a few cells from the point of decay. Thus α-emitters are ideal for treating small-volume, homogeneous, disseminated cancer (Baidoo et al. 2013). Despite their advantageous radiochemical and radiopharmaceutical properties, the number of α particle emitting diagnostic and therapeutic drugs is much lower than those of the β particle emitting ones. The α emitter [^{223}Ra]RaCl (Alpharadin) and other Ra-223 containing radiopharmaceuticals have shown efficacy in castrate-resistant prostate and bone cancer (Shirley et al. 2014; Zustovich et al. 2014). Ra-223 mimics calcium depositing in skeletal tissue, and disposes low hematologic toxicity. At present, this radionuclide is the only drug that facilitates overall survival in patients with bone metastases and prostate cancer, and improves patient prognosis (Zustovich et al. 2014).

A number of immune-conjugates that incorporate emitters and DTPA or DOTA chelators, have shown therapeutic opportunities. For example, Bi-213 coupled to an anti-CD33 antibody (HuM195, lintuzumab), was tested in a phase I clinical trial of patients with acute myeloid leukemia who had been pre-sensitized with cytarabine (Rosenblat et al. 2010). In spite of their effectiveness and the new generation bifunctional Bi-212/213 derivatives that have been recently developed, the short half-life of the radionuclides and their slow complexation kinetics, remain an unsolved problem (Hassfjell et al. 2001). To overcome these issues, novel octadentate chelator (4-[2-(bis-carboxymethyl-amino)-ethyl]-7-carboxymethyl-acetic acid) (NETA) containing derivatives are being developed that have shown increased *in vitro* serum stability, biodistribution and tumor uptake in a preclinical study (Kang et al. 2013).

Another α emitter-containing radiotherapeutics, At-211 labelled immune-conjugates have been synthesized and evaluated for their therapeutic potential (Zalutsky et al. 2007, 2008). Since proteins labelled with At-211 by direct electrophilic astatination were unstable following *in vivo* administration (Zalutsky et al. 1996), N-succinimidyl-3-[^{211}At] astatobenzoate (SAB) and other formulation strategies has been considered (Pozzi et al. 2005a; Pozzi et al. 2005b). The therapeutic potential and utility of MAbs and MAb fragments labelled with At-211 has been investigated in several MAb systems (Eriksson et al. 2013; Zalutsky et al. 2007). Although, studies on [^{211}At]MAbs following intravenous administration demonstrate site-specific accumulation in tumors, increased levels of At-211 in normal tissues indicates rapid rates of At-211 metabolism (radiolytic factors). In spite of this fact, the *in vivo* stability of radioimmuno-conjugates labelled with [^{211}At] SAB may be acceptable, particularly for non-intravenous applications.

An experimental development of the targeted therapy is the boron neutron capture therapy (Moss 2014) that uses B-10 which concentrates in malignant brain tumors. After administration of the B-10 containing pharmaceutical, that is the precursor of the α emitting radiopharmaceutical, the

patient is irradiated with thermal neutrons. These neutrons are strongly absorbed by B-10, producing high-energy α particles in an (n,α) reaction, which kill the cells where the B-10 containing precursor accumulated. The disadvantage of this procedure is that the patient is required to be brought to a nuclear reactor, rather than the radioisotopes being taken to the patient.

β Particle emitting radiopharmaceuticals and their therapeutic use

Radionuclides such as P-32, Cu-64/67, Sr-89, Y-90, Sn-117m, I-131, Rh-105, Ho-166, Lu-177 and Re-186/188 that decay by β emission are used most extensively for radiotherapeutic applications in current clinical practice (Volkert et al. 1999). β Particles produce a highly homogenous radiation dose, sparsely ionize molecules with a linear energy transfer value of about 0.2 keV/mm, and have a range of several millimeters in solid tissue. One consequence of this relatively long range is that radionuclides, especially with high energy electrons, are able to cross-fire neighbouring, non-targeted tissue components. This phenomenon proved to be particularly detrimental for tumors of the bone marrow since collateral irradiation of this tissue leads to myelosuppression and limits therapeutic application of high energy emitters (Bayouth et al. 1995; Johnson et al. 1992; Volkert et al. 1993). To circumvent this problem, a new concept, the combination of different isotopes with high (Y-90) and low (Lu-177) energy β emission, has proved to be a successful approach in the treatment of tumors and their micro-metastases in rat tumor models (de Jong et al. 2005).

The potential of radiolabelled antibodies, radioimmunoconjugates, to deliver a therapeutic dose of radiation to malignant cells has been particularly well documented in the case of lymphomas and neuroblastoma (Barbet et al. 2012). Currently, two drugs, anti-CD20 antibodies labelled with Y-90 (ibritumomabtiuxetan; Zevalin) or I-131 (tositumomab; Bexxar) have shown efficacy in B-cell non-Hodgkin lymphoma (Witzig et al. 2011). These agents are also used as supplement following chemotherapy (Witzig 2013). Recently, other cell surface antigens, including the CD45, CD66 and CD33, have also been targeted with β-emitting radioimmunoconjugates for the treatment of haematological malignancies (Buchmann et al. 2009).

As has been shown, I-131 has a very high radiotherapeutic potential for the treatment of malignant diseases such as gliomas, pheochromocytoma, and carcinoids. I-131 is commonly used to treat thyroid cancer, and also to treat non-malignant thyroid disorders. It is also used for imaging and therapy of neuroblastomas (Wilson et al. 2014). Most neuroblastomas express a noradrenaline transporter that can take up [^{131}I]meta-iodobenzylguanidine (mIBG), a structural analogue of norepinephrine (Rufini et al. 2013). Generally, [^{131}I]mIBG doses used to vary between 100 and 200 mCi (3.7-7.4 GBq) and are administered intravenously for systemic therapy, presensitization for chemotherapy, consolidation with myeloablative chemotherapy and minimal residual disease treatment with immune- and differentiation therapy. Its most significant therapeutic drawbacks are the radiation-induced bone marrow suppression and the low tumor to non-target ratio. To overcome these disadvantages, the use of At-211 has proved to be a successful approach. *In vitro* cytotoxic results with this analogue on three different neuroblastoma cell lines have suggested that [^{211}At]mABG could be a good substitute of the mIBG analogue (Strickland et al. 1994).

The treatment of bone cancer has always been a challenge due to the concomitant bone marrow suppression present. From therapeutic viewpoint, [^{89}Sr]$SrCl_2$ (Metastron) and Sm-153 EDTMP (Quadramet) are the most widely used radiopharmaceuticals for metastatic bone cancers (Baczyk et al. 2007; McEwan et al. 1994). Nowadays, the use of [^{32}P] sodium orthophosphate and [^{32}P]phosphate is only limited to a few cases, and are more important for myeloid bone cancer associated palliative therapy (Roberts, Jr. 1979; Tennvall et al. 2007). However, the use of P-32 conjugates has been emerged in the treatment of various malignant intracavitary tumors. Interestingly, the [^{32}P]chromic phosphate colloid has been approved for the treatment of metastatic ovarian, renal and GI cancers in spite of the fact that this colloid does not really discriminate between tumorous and non-tumorous tissue (Denis-Bacelar et al. 2013; Pattillo et al. 1995; Zubillaga et al. 1996). This drawback limits its widespread application, thus this colloid compound has been substituted with tumor-specific antibodies labelled with I-131, Y-90 or Lu-177 that have higher selectivity for the target tissue (Deutsch et al. 1993; Meredith et al. 1996).

The mechanism of action of these radiopharmaceuticals relies on reductive processes, trans-metallation or direct adsorption on the inorganic, hydroxyapatite component of the regenerating bone. The rate and extent of these reactions depends on the kinetic and thermodynamic stability of the complexes. Re-186 HEDP and Sn-117m DTPA radionuclide complexes are two other therapeutic agents that are used for the eradication of bone cancer. The Sn-117m DTPA chelate is an experimental radiopharmaceutical undergoing clinical evaluation for the treatment of painful bone metastases (Pandit-Taskar et al. 2004). Re-186 HEDP is a potentially useful radiopharmaceutical as clinical studies have shown encouraging results in palliative therapy where an overall response rate of 70% in painful bone metastases was measured (Lam et al. 2004; Syed et al. 2006).

Auger-electron emitting radionuclides and their therapeutic use

Radionuclides such as I-125, I-123 and In-111, which possess

abundance of protons and decay by electron capture, are well suited to targeted radiotherapy. They emit short-range (<1 nm to a few mm), low-energy (<1 keV), high linear energy transfer (4 - 26 keV/mm) Auger electrons that cause intense energy deposition in a nanometer scale volume around the site of decay (Kassis 2011). Cross-fire events are limited and non-specific radiotoxicity thus avoided. In general, Auger electron-emitting isotopes are most effective when incorporated into or localized in close proximity to DNA. Efficient systems for directing Auger electron-emitting isotopes specifically to the nuclei of cancer cells are being searched extensively (Cornelissen et al. 2010, 2012b; Lobachevsky et al. 2005; Smit et al. 2001). A potential for future therapeutic benefit in the administration of Auger electron-emitting isotopes has been suggested by only a small number of clinical studies. A combination of intrathecal [^{125}I]5-iodo-2'-deoxuyridine ([^{125}I] IUdR) with methotrexate resulted in a fall in CA 19-9 tumor marker antigene, and clinical improvement in a patient with pancreatic cancer with meningeal metastases (Rebischung et al. 2008).

Tumor pre-targeting

Normal tissue toxicity, especially to the bone marrow is the major limiting factor in the application of radio-immunotherapy to solid tumors. Attempts have been made towards the improvement of biodistribution of radiopharmaceuticals, such as the use of a secondary antibody, local delivery or the use of metabolisable linkers. One of the approaches that facilitates high tumor uptake of therapeutic radionuclides and provides rapid clearance from blood and non-target tissues, is defined as "tumor pre-targeting" (Goldenberg et al. 2007; Sharkey et al. 2005). Several pre-targeting strategies have been worked out, but the most well known is based on the avidin/streptavidin biotin system (Casalini et al. 1997; Li et al. 2005; Wilbur et al. 2002). Since the early development of this approach many pre-targeting systems, such as bispecific anticancer antibodies with radiolabelled peptide haptens have been developed (Goldenberg et al. 2007). The avidin/streptavidin biotin system is attractive since the affinity of avidin or streptavidin to biotin is very high. Pre-targeting uses a three-step approach wherein three reagents are administered sequentially in a protocol, designed to maximize the tumor radiation dose in the target tissue (Fig. 12).

The first step is a pre-sensitization of the target cancer cells with a long-lived, high affinity and specificity circulating non-radiolabelled MAb (e.g., avidin/steptavidin-MAb or bivalent MAb). Once the MAb construct has been localized in the tumor, a so called "chase molecule" is given in the second step at peak tumor uptake to eliminate the unbound MAb construct from the blood and other non-target tissues. The third step involves the administration of a radiolabelled (usually Y-90, I-131, Re-188 or Cu-67) hapten or biotin conjugate. Maximum tumor concentrations and tumor to non-target ratios are achieved in ca. 1-3 h. There is long-term retention of radioactivity associated with the streptavidin-MAb conjugate in the tumor (*i.e.*, days), while the rapid elimination of unlocalized radioactivity attached to the small effector molecule, greatly reduces radiation dose to normal tissues (Schoffelen et al. 2013).

Summary and future perspectives

The patient outcomes resulting from the use of radiopharmaceuticals have demonstrated the value of these agents in tumor diagnosis and in the treatment of diffuse, otherwise non-treatable conditions. Despite recent advances in biology, combinatorial-, peptide- and radiochemistry, only a limited number of radiolabelled drugs are used routinely for diagnosis and therapy. The greatest challenge associated with the design of novel radiolabelled compounds is the development of radiolabelled conjugates that have the ability for selective tissue targeting and that meet the therapeutic requirements with an acceptable toxicity. Ideal therapeutic radiopharmaceuticals should locate at the tumor site, producing minimal or tolerable radiation damage to normal surrounding tissues. It is difficult to achieve due to a variety of factors that are related to the chemical and physico-chemical characteristics of the radiopharmaceutical. The design of better radiotherapeutic agents, thus, requires optimization between specific *in vivo* targeting of the tumor and the clearance of radioactivity from non-target radiosensitive tissues as well as the decay properties of the radionuclide. The continuous radiopharmaceutical development is in progress because molecular imaging has enormous potential for early detection of diseases. Nowadays, multi-modality imaging, a combination of nuclear medicine and radiology, is beginning to gain widespread application. It offers not only more accurate diagnosis, but also facilitates personalized therapy and helps a better understanding of the underlying pathological processes.

Abbreviations

CCK - cholecystokinin; CT - computer tomography; DNA - deoxynucleic acid; ^{18}F-DOPA - [^{18}F]3,4-dihydroxy-6-fluoro-L-phenylalanine; DOTA - 1.4.7.10-cyclododecyltetraacetic acid; DOTMP - 1,4,7,10-cyclododecyltetraaminetetramethylenephosphonic acid; DTPA - diethylenetriaminepentaacetic acid; DTPMP - diethylenetriaminepenta(methylenephosphonic acid); EDTA - ethylenediaminetetraacetic acid; EDTMP - ethylenediaminetetra(ethylenephosphonic acid); EEG - electroencephalography; EUBED - equivalent uniform biologically

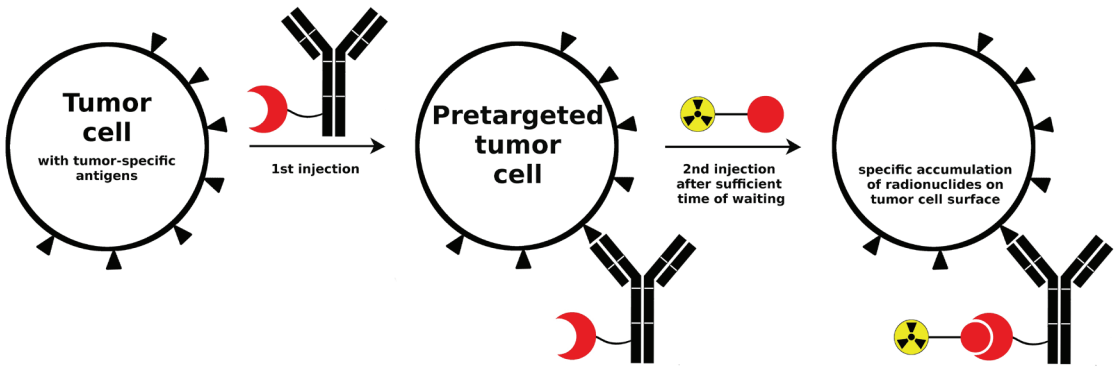

Figure 12. Pre-targeting starts with a pre-sensitization of the tumor cell with avidin/streptavidin-MAb or bivalent MAb complex that is followed by the addition of the radiolabelled hapten or biotin conjugate. The latter provides cytotoxic dose of irradiation that eventually kills the tumor cell.

effective dose; FDG - fluoro-2-deoxy-D-glucose; FET - *O*-(2-fluoroethyl)-L-tyrosine; FLT - 3'-deoxy-3'-fluorothymidine; GLP-1R - glucagon-like peptide-1 receptor; GRPR - gastrin-releasing peptide receptor; HEDP - 1-hydroxyethylidene-1, 1-diphosphonic acid; IMT - iodo-α-methyl tyrosine; IudR - 5-iodo-2'-deoxuyridine; MAb - monoclonal antibody; MC1-R - melanocortin-1 receptor; MEG - magnetoencephalography; mIBG - meta-iodobenzylguanidine; MIRD - medical internal radiation dose; MRI - magnetic resonance imaging; NETA - 4-[2-(bis-carboxymethyl-amino)-ethyl]-7-carboxymethyl-acetic acid; NTA - nitrilotriacetic acid; NTMP - nitrilotrimethylenephosphonic acid; PET - positron emission tomography; SAB - N-succinimidyl-3-astatobenzoate; SPECT - single photon emission computer tomography; TOC - D-Phe-c(Cys-Tyr-D-Trp-Lys-Thr-Cys)-Thr(ol)).

Acknowledgment

Financial support from the Hungarian National Development Agency (TÁMOP 4.2.2.A-11/1/KONV-2012-0052) and the János Bolyai Research Scholarship of the Hungarian Academy of Sciences (Cs.T. and B.A.) are acknowledged.

References

Aerts A, Impens N, Gijs M, D'Huyvetter M, Vanmarcke H, Ponsard B, Lahoutte T, Luxen A, Baatout S (2014) Biological Carrier Molecules of Radiopharmaceuticals for Molecular Cancer Imaging and Targeted Cancer Therapy. Curr Pharm Des 20:5218-5244.

Anderson CD (1932) The apparent existence of easily deflectable positives. Science 76:238-239.

Anger HO (1952) Use of a gamma-ray pinhole camera for in vivo studies. Nature 170:200-201.

Asabella AN, Cascini GL, Altini C, Paparella D, Notaristefano A, Rubini G (2014) The copper radioisotopes: a systematic review with special interest to ^{64}Cu. Biomed Res Int 2014:786463.

Attard AR, Chappell MJ, Bradwell AR (1995) Model based calculation for effective cancer radioimmunotherapy. Br J Radiol 68:636-645.

Baczyk M, Czepczynski R, Milecki P, Pisarek M, Oleksa R, Sowinski J (2007) ^{89}Sr versus ^{153}Sm-EDTMP: comparison of treatment efficacy of painful bone metastases in prostate and breast carcinoma. Nucl Med Commun 28:245-250.

Baidoo KE, Yong K, Brechbiel MW (2013) Molecular pathways: targeted alpha-particle radiation therapy. Clin Cancer Res 19: 530-537.

Barbet J, Bardies M, Bourgeois M, Chatal JF, Cherel M, Davodeau F, Faivre-Chauvet A, Gestin JF, Kraeber-Bodere F (2012) Radiolabeled antibodies for cancer imaging and therapy. Methods Mol Biol 907:681-697.

Bayouth JE, Macey DJ, Kasi LP, Garlich JR, McMillan K, Dimopoulos MA, Champlin RE (1995) Pharmacokinetics, dosimetry and toxicity of holmium-166-DOTMP for bone marrow ablation in multiple myeloma. J Nucl Med 36:730-737.

Blumgart HL, Yens OC (1926) Studies on the velocity of blood flow: I. The method utilized. J Clin Invest 4:1-13.

Bodei L, Handkiewicz-Junak D, Grana C, Mazzetta C, Rocca P, Bartolomei M, Lopera SM, Cremonesi M, Chinol M, Macke HR, Paganelli G (2004) Receptor radionuclide therapy with ^{90}Y-DOTATOC in patients with medullary thyroid carcinomas. Cancer Biother Radiopharm 19:65-71.

Bodei L, Mueller-Brand J, Baum RP, Pavel ME, Horsch D, O'Dorisio MS, O'Dorisio TM, Howe JR, Cremonesi M, Kwekkeboom DJ, Zaknun JJ (2013) The joint IAEA, EANM, and SNMMI practical guidance on peptide receptor radionuclide therapy (PRRNT) in neuroendocrine tumours. Eur J Nucl Med Mol Imaging 40:800-816.

Bolzati C, Boschi A, Uccelli L, Tisato F, Refosco F, Cagnolini A, Duatti A, Prakash S, Bandoli G, Vittadini A (2002) Chemistry of the strong electrophilic metal fragment [(99) Tc(N)(PXP)](2+) (PXP = diphosphine ligand). A novel tool for the selective labeling of small molecules. J Am Chem Soc 124:11468-11479.

Boschi A, Bolzati C, Uccelli L, Duatti A, Benini E, Refosco F, Tisato F, Piffanelli A (2002) A class of asymmetrical nitrido ^{99m}Tc heterocomplexes as heart imaging agents with improved biological properties. Nucl Med Commun 23:689-693.

Boschi A, Uccelli L, Bolzati C, Duatti A, Sabba N, Moretti E, Di Domenico G, Zavattini G, Refosco F, Giganti M (2003) Synthesis and biologic evaluation of monocationic asymmetric ^{99m}Tc-nitride heterocomplexes showing high heart uptake and improved imaging properties. J Nucl Med 44:806-814.

Boyd GS, Merrick MV, Monks R, Thomas IL (1981) Se-75 Labeled bile acid analogs, new radiopharmaceuticals for investigatin the enterohepatic circulation. J Nucl Med 22:720-725.

Brans B, Bodei L, Giammarile F, Linden O, Luster M, Oyen WJ, Tennvall J (2007) Clinical radionuclide therapy dosimetry: the quest for the "Holy Gray". Eur J Nucl Med Mol Imaging 34:772-786.

Bristow MR, Ginsburg R, Minobe W, Cubicciotti RS, Sageman WS, Lurie K, Billingham ME, Harrison DC, Stinson EB (1982) Decreased catecholamine sensitivity and beta-adrenergic-receptor density in failing human hearts. N Engl J Med 307:205-211.

Buchmann I, Meyer RG, Mier W, Haberkorn U (2009) Myeloablative radioimmunotherapy in conditioning prior to haematological stem cell transplantation: closing the gap between benefit and toxicity? Eur J Nucl Med Mol Imaging 36:484-498.

Cai LS, Lu SY, Pike VW (2008) Chemistry with [F-18]fluoride ion. Eur J Org Chem 17:2853-2873.

Casalini P, Luison E, Menard S, Colnaghi MI, Paganelli G, Canevari S (1997) Tumor pretargeting: role of avidin/streptavidin on monoclonal antibody internalization. J Nucl Med 38:1378-1381.

Chadwick J (1932) The existence of a neutron. Proc Roy Soc 136:692-708.

Chen W (2007) Clinical applications of PET in brain tumors. J Nucl Med 48:1468-1481.

Chianelli M, Signore A, Mansi L, Salvatori M (2011) Time for radiobiology in the nuclear medicine community. Eur J Nucl Med Mol Imaging 38:1267-1269.

Chiewitz O, Hevesy G (1935) Radioactive indicators in the study of phosphorus metabolism in rats. Nature 136:754-755.

Choppin G, Liljenzin, J.-O, and Rydberg, J (2002) Radiochemistry and nuclear chemistry. Butterworth-Heinemann, Woburn, MA, USA.

Clifford RB (2014) Perspectives in molecular imaging through translational research, human medicine, and veterinary medicine. Semin Nucl Med 44:66-75.

Cornelissen B, Vallis KA (2010) Targeting the nucleus: an overview of Auger-electron radionuclide therapy. Curr Drug Discov Technol 7:263-279.

Cornelissen B, Darbar S, Kersemans V, Allen D, Falzone N, Barbeau J, Smart S, Vallis KA (2012a) Amplification of DNA damage by a gammaH2AX-targeted radiopharmaceutical. Nucl Med Biol 39:1142-1151.

Cornelissen B, Waller A, Target C, Kersemans V, Smart S, Vallis KA (2012b) ^{111}In-BnDTPA-F3: an Auger electron-emitting radiotherapeutic agent that targets nucleolin. Eur J Nucl Med Mol Imaging 20:9.

Coutard H (1937) The results and methods of treatment of cancer by radiation. Ann Surg 106:584-598.

Czisch M, Wehrle R, Kaufmann C, Wetter TC, Holsboer F, Pollmacher T, Auer DP (2004) Functional MRI during sleep: BOLD signal decreases and their electrophysiological correlates. Eur J Neurosci 20:566-574.

Dash A, Knapp FF, Pillai MR (2013) Targeted radionuclide therapy--an overview. Curr Radiopharm 6:152-180.

de Jong M, Breeman WA, Valkema R, Bernard BF, Krenning EP (2005) Combination radionuclide therapy using ^{177}Lu- and ^{90}Y-labeled somatostatin analogs. J Nucl Med 46 Suppl 1:13S-17S.

Deleporte A, Flamen P, Hendlisz A (2010) State of the art: radiolabeled microspheres treatment for liver malignancies. Expert Opin Pharmacother 11:79-586.

Denis-Bacelar AM, Romanchikova M, Chittenden S, Saran FH, Mandeville H, Du Y, Flux GD (2013) Patient-specific dosimetry for intracavitary ^{32}P-chromic phosphate colloid therapy of cystic brain tumours. Eur J Nucl Med Mol Imaging 40:1532-1541.

Deutsch E, Brodack JW, Deutsch KF (1993) Radiation synovectomy revisited. Eur J Nucl Med 20:1113-1127.

Di Pasqua AJ, Yuan H, Chung Y, Kim JK, Huckle JE, Li C, Sadgrove M, Tran TH, Jay M, Lu X (2013) Neutron-activatable holmium-containing mesoporous silica nanoparticles as a potential radionuclide therapeutic agent for ovarian cancer. J Nucl Med 54:111-116.

Dolle F (2013) Carbon-11 and fluorine-18 chemistry devoted to molecular probes for imaging the brain with positron emission tomography. J Labelled Comp Radiopharm 56:65-67.

Dong C, Liu Z, Wang F (2014) Peptide-based radiophar-

maceuticals for targeted tumor therapy. Curr Med Chem 21:139-152.

Eberlein U, Broer JH, Vandevoorde C, Santos P, Bardies M, Bacher K, Nosske D, Lassmann M (2011) Biokinetics and dosimetry of commonly used radiopharmaceuticals in diagnostic nuclear medicine - a review. Eur J Nucl Med Mol Imaging 38:2269-2281.

Ell PJ (2014) The contribution of medical physics to nuclear medicine: a physician's perspective. EJNMMI Physics 1:3.

Eriksson SE, Back T, Elgstrom E, Jensen H, Nilsson R, Lindegren S, Tennvall J (2013) Successful radioimmunotherapy of established syngeneic rat colon carcinoma with ^{211}At-mAb. Eur J Nucl Med Mol Imaging 3:23.

Fani M, Maecke HR (2012a) Radiopharmaceutical development of radiolabelled peptides. Eur J Nucl Med Mol Imaging 39:S11-S30.

Fani M, Maecke HR, Okarvi SM (2012b) Radiolabeled peptides: valuable tools for the detection and treatment of cancer. Theranostics 2:481-501.

Ferro-Flores G, Ocampo-Garcia BE, Santos-Cuevas CL, Morales-Avila E, Azorin-Vega E (2014) Multifunctional radiolabeled nanoparticles for targeted therapy. Curr Med Chem 21:124-138.

Forero A, Meredith RF, Khazaeli MB, Shen S, Grizzle WE, Carey D, Busby E, LoBuglio AF, Robert F (2005) Phase I study of 90Y-CC49 monoclonal antibody therapy in patients with advanced non-small cell lung cancer: effect of chelating agents and paclitaxel co-administration. Cancer Biother Radiopharm 20:467-478.

Forrer F, Waldherr C, Maecke HR, Mueller-Brand J (2006) Targeted radionuclide therapy with 90Y-DOTATOC in patients with neuroendocrine tumors. Anticancer Res 26:703-707.

Giovacchini G, Picchio M, Scattoni V, Garcia PR, Briganti A, Gianolli L, Montorsi F, Messa C (2010) PSA doubling time for prediction of [(11)C]choline PET/CT findings in prostate cancer patients with biochemical failure after radical prostatectomy. Eur J Nucl Med Mol Imaging 37:1106-1116.

Goins BA (2008) Radiolabeled lipid nanoparticles for diagnostic imaging. Expert Opin Med Diagn 2:853-873.

Goldenberg DM, Chatal JF, Barbet J, Boerman O, Sharkey RM (2007) Cancer imaging and therapy with bispecific antibody pretargeting. Update Cancer Ther 2:19-31.

Grosu AL, Astner ST, Riedel E, Nieder C, Wiedenmann N, Heinemann F, Schwaiger M, Molls M, Wester HJ, Weber WA (2011) An interindividual comparison of O-(2-[18F] fluoroethyl)-L-tyrosine (FET)- and L-[methyl-11C]methionine (MET)-PET in patients with brain gliomas and metastases. Int J Radiat Oncol Biol Phys 81:1049-1058.

Häfeli UO (2001) Focus on biotechnology. Kluwer Academic Publishing, Dordrecht.

Hamilton JG, Stone RS (1937) The intravenous and intraduodenal administration of radio-sodium. Radiology 28: 78-188.

Harbert JC and Ziessman HA (1987) Therapy with intraarterial microspheres. Raven Press, New York.

Hassfjell S, Brechbiel MW (2001) The development of the alpha-particle emitting radionuclides ^{212}Bi and ^{213}Bi, and their decay chain related radionuclides, for therapeutic applications. Chem Rev 101:2019-2036.

Haug AR, Auernhammer CJ, Wangler B, Schmidt GP, Uebleis C, Goke B, Cumming P, Bartenstein P, Tiling R, Hacker M (2010) 68Ga-DOTATATE PET/CT for the early prediction of response to somatostatin receptor-mediated radionuclide therapy in patients with well-differentiated neuroendocrine tumors. J Nucl Med 51:1349-1356.

Hertz S, Roberts A, Evans RD (1938) Radioactive iodine as an indicator in the study of thyroid physiology. Proc Soc Exp Biol Med 38:510-513.

Hevesy G (1923) The absorption and translocation of lead by plants. Biochem J 4:439-445.

Higley B, Smith FW, Smith T, Gemmell HG, Das GP, Gvozdanovic DV, Graham D, Hinge D, Davidson J, Lahiri A (1993) Technetium-99m-1,2-bis[bis(2-ethoxyethyl) phosphino]ethane: human biodistribution, dosimetry and safety of a new myocardial perfusion imaging agent. J Nucl Med 34:30-38.

Hong SY, Tobias G, Al Jamal KT, Ballesteros B, Ali-Boucetta H, Lozano-Perez S, Nellist PD, Sim RB, Finucane C, Mather SJ, Green ML, Kostarelos K, Davis BG (2010) Filled and glycosylated carbon nanotubes for in vivo radioemitter localization and imaging. Nat Mater 9:485-490.

Hu M, Chen P, Wang J, Scollard DA, Vallis KA, Reilly RM (2007) 123I-labeled HIV-1 tat peptide radioimmunoconjugates are imported into the nucleus of human breast cancer cells and functionally interact in vitro and in vivo with the cyclin-dependent kinase inhibitor, p21(WAF-1/Cip-1). Eur J Nucl Med Mol Imaging 34:368-377.

Jacobson AF, Senior R, Cerqueira MD, Wong ND, Thomas GS, Lopez VA, Agostini D, Weiland F, Chandna H, Narula J (2010) Myocardial iodine-123 meta-iodobenzylguanidine imaging and cardiac events in heart failure. Results of the prospective ADMIRE-HF (AdreView Myocardial Imaging for Risk Evaluation in Heart Failure) study. J Am Coll Cardiol 55:2212-2221.

Jánoki GA, Kerekes A (1992) Pharmacokinetics of radiopharmaceuticals. Acta Physiol Hung 79:183-196.

Johnson JC, Langhorst SM, Loyalka SK, Volkert WA, Ketring AR (1992) Calculation of radiation dose at a bone-to-marrow interface using Monte Carlo modeling techniques (EGS4). J Nucl Med 33:623-628.

Johnson LL, Seldin DW (1990) Clinical experience with technetium-99m teboroxime, a neutral, lipophilic myocardial

perfusion imaging agent. Am J Cardiol 66:63E-67E.
Joliot F, Curie I (1934) Artificial production of a new kind of radio-element. Nature 133:201-202.
Jones AG, Abrams MJ, Davison A, Brodack JW, Toothaker AK, Adelstein SJ, Kassis AI (1984) Biological studies of a new class of technetium complexes: the hexakis(alkylisonitrile)technetium(I) cations. Int J Nucl Med Biol 11:225-234.
Jones RL, Sproule BJ, Overton TR (1978) Measurement of regional ventilation and lung perfusion with Xe-133. J Nucl Med 19:1187-1188.
Kaltsas GA, Papadogias D, Makras P, Grossman AB (2005) Treatment of advanced neuroendocrine tumours with radiolabelled somatostatin analogues. Endocr Relat Cancer 12:683-699.
Kam BLR, Teunissen JJM, Krenning EP, de Herder WW, Khan S, van Vliet EI, Kwekkeboom DJ (2012) Lutetium-labelled peptides for therapy of neuroendocrine tumors. Eur J Nucl Med Mol Imaging 39:S103-S112.
Kang CS, Song HA, Milenic DE, Baidoo KE, Brechbiel MW, Chong HS (2013) Preclinical evaluation of NETA-based bifunctional ligand for radioimmunotherapy applications using ^{212}Bi and ^{213}Bi: radiolabeling, serum stability, and biodistribution and tumor uptake studies. Nucl Med Biol 40:600-605.
Kassis AI (2011) Molecular and cellular radiobiological effects of Auger emitting radionuclides. Radiation Protection Dosimetry 143:241-247.
Kersemans V, Kersemans K, Cornelissen B (2008) Cell penetrating peptides for in vivo molecular imaging applications. Curr Pharm Des 14:2415-2447.
Koehler L, Gagnon K, McQuarrie S, Wuest F (2010) Iodine-124:a promising positron emitter for organic PET chemistry. Molecules 15:2686-2718.
Kowalsky, RJ and Falen, SW (2011) Radiopharmaceuticals in nuclear pharmacy and nuclear medicine. American Pharmacists Association, Washington DC.
Lam MG, de Klerk JM, van Rijk PP (2004) ^{186}Re-HEDP for metastatic bone pain in breast cancer patients. Eur J Nucl Med Mol Imaging 31 S1:S162-S170.
Lassmann M, Chiesa C, Flux G, Bardies M (2011) EANM Dosimetry Committee guidance document: good practice of clinical dosimetry reporting. Eur J Nucl Med Mol Imaging 38:192-200.
Laufer EM, Winkens HM, Corsten MF, Reutelingsperger CP, Narula J, Hofstra L (2009) PET and SPECT imaging of apoptosis in vulnerable atherosclerotic plaques with radiolabeled Annexin A5. Q J Nucl Med Mol Imaging 53:26-34.
Lawrence EO, Livingstone MS (1932) Production of high speed light ions without the use of high voltages. Phys Rev 40:19-35.
Li GP, Zhang H, Zhu CM, Zhang J, Jiang XF (2005) Avidin-biotin system pretargeting radioimmunoimaging and radioimmunotherapy and its application in mouse model of human colon carcinoma. World J Gastroenterol 11:6288-6294.
Lobachevsky PN, Martin RF (2005) DNA breakage by decay of Auger electron emitters: experiments with ^{123}I-iodoHoechst 33258 and plasmid DNA. Radiat Res 164:766-773.
Marshall B. (1990) A chronology of nuclear medicine. Heritage Publications, London.
Marti-Bonmati L, Sopena R, Bartumeus P, Sopena P (2010) Multimodality imaging techniques. Contrast Media Mol Imaging 5:180-189.
Martinez-Montes E, Valdes-Sosa PA, Miwakeichi F, Goldman RI, Cohen MS (2004) Concurrent EEG/fMRI analysis by multiway Partial Least Squares. Neuroimage 22:1023-1034.
McEwan AJ, Amyotte GA, McGowan DG, MacGillivray JA, Porter AT (1994) A retrospective analysis of the cost effectiveness of treatment with Metastron (^{89}Sr-chloride) in patients with prostate cancer metastatic to bone. Nucl Med Commun 15:499-504.
Meredith RF, Partridge EE, Alvarez RD, Khazaeli MB, Plott G, Russell CD, Wheeler RH, Liu T, Grizzle WE, Schlom J, LoBuglio AF (1996) Intraperitoneal radioimmunotherapy of ovarian cancer with lutetium-177-CC49. J Nucl Med 37:1491-1496.
Milenic DE, Garmestani K, Brady ED, Albert PS, Ma D, Abdulla A, Brechbiel MW (2005) α-Particle radioimmunotherapy of disseminated peritoneal disease using a ^{212}Pb-labeled radioimmunoconjugate targeting HER2. Cancer Biother Radiopharm 20:557-568.
Miller PW, Long NJ, Vilar R, Gee AD (2008) Synthesis of ^{11}C, ^{18}F, ^{15}O, and ^{13}N radiolabels for positron emission tomography. Angew Chem Int Ed Engl 47:8998-9033.
Mishra A, Lai GH, Schmidt NW, Sun VZ, Rodriguez AR, Tong R, Tang L, Cheng J, Deming TJ, Kamei DT, Wong GC (2011) Translocation of HIV TAT peptide and analogues induced by multiplexed membrane and cytoskeletal interactions. Proc Natl Acad Sci USA 108:16883-16888.
Mitterhauser M, Wadsak W (2014) Imaging biomarkers or biomarker imaging? Pharmaceuticals 7:765-778.
Moss RL (2014) Critical review, with an optimistic outlook, on boron neutron capture therapy (BNCT). Appl Radiat Isot 88:2-11.
Muller JH, Rossier PH (1951) A new method for the treatment of cancer of the lungs by means of artificial radioactivity. Acta radiol 35:449-468.
Nagren K, Halldin C, Muller L, Swahn CG, Lehikoinen P (1995) Comparison of [^{11}C]methyl triflate and [^{11}C] methyl iodide in the synthesis of PET radioligands such as [^{11}C]beta-CIT and [^{11}C]beta-CFT. Nucl Med Biol

22:965-979.

Nasrallah I, Dubroff J (2013) An overview of PET neuroimaging. Semin Nucl Med 43:449-461.

Ogawa K, Mukai T, Asano D, Kawashima H, Kinuya S, Shiba K, Hashimoto K, Mori H, Saji H (2007) Therapeutic effects of a ^{186}Re-complex-conjugated biphosphonate for the palliation of metastatic bone pain in an animal model. J Nucl Med 48:122-127.

Okarvi SM (2008) Peptide-based radiopharmaceuticals and cytotoxic conjugates: potential tools against cancer. Cancer Treat Rev 34:13-26.

Pafundi DH, Laack NN, Youland RS, Parney IF, Lowe VJ, Giannini C, Kemp BJ, Grams MP, Morris JM, Hoover JM, Hu LS, Sarkaria JN, Brinkmann DH (2013) Biopsy validation of ^{18}F-DOPA PET and biodistribution in gliomas for neurosurgical planning and radiotherapy target delineation: results of a prospective pilot study. Neuro Oncol 15:1058-1067.

Paganelli G, Bodei L, Junak DH, Rocca P, Papi S, Sierra ML, Gatti M, Chinol M, Bartolomei M, Fiorenza M, Grana C (2002) Y-90-DOTA-D-Phe(1)-Try(3)-octreotide in therapy of neuroendocrine malignancies. Biopolymers 66:393-398.

Palumbo B (2008) Brain tumour recurrence: brain single-photon emission computerized tomography, PET and proton magnetic resonance spectroscopy. Nucl Med Commun 29:730-735.

Palumbo B, Buresta T, Nuvoli S, Spanu A, Schillaci O, Fravolini ML, Palumbo I (2014) SPECT and PET serve as molecular imaging techniques and in vivo biomarkers for brain metastases. Int J Mol Sci 15:9878-9893.

Pandit-Taskar N, Batraki M, Divgi CR (2004) Radiopharmaceutical therapy for palliation of bone pain from osseous metastases. J Nucl Med 45:1358-1365.

Pattillo RA, Collier BD, Abdel-Dayem H, Ozker K, Wilson C, Ruckert AC, Hamilton K (1995) Phosphorus-32-chromic phosphate for ovarian cancer: I. Fractionated low-dose intraperitoneal treatments in conjunction with platinum analog chemotherapy. J Nucl Med 36:29-36.

Patton DD (2003) The birth of nuclear medicine instrumentation: Blumgart and Yens, 1925. J Nucl Med 44:1362-1365.

Platts EA, North TL, Pickett RD, Kelly JD (1995) Mechanism of uptake of technetium-tetrofosmin. I: Uptake into isolated adult rat ventricular myocytes and subcellular localization. J Nucl Cardiol 2:317-326.

Pozzi OR, Zalutsky MR (2005a) Radiopharmaceutical chemistry of targeted radiotherapeutics, part 1: effects of solvent on the degradation of radiohalogenation precursors by ^{211}At alpha-particles. J Nucl Med 46:700-706.

Pozzi OR, Zalutsky MR (2005b) Radiopharmaceutical chemistry of targeted radiotherapeutics, Part 2: radiolytic effects of ^{211}At alpha-particles influence *N*-succinimidyl 3-^{211}At-astatobenzoate synthesis. J Nucl Med 46:1393-1400.

Pusey WA (1900) Roentgen-rays in the treatment of skin diseases and for the removal of hair. The Journal of Cutaneous Diseases Including Syphilis 18:302-318.

Reardon DA, Akabani G, Coleman RE, Friedman AH, Friedman HS, Herndon JE, Cokgor I, McLendon RE, Pegram CN, Provenzale JM, Quinn JA, Rich JN, Regalado LV, Sampson JH, Shafman TD, Wikstrand CJ, Wong TZ, Zhao XG, Zalutsky MR, Bigner DD (2002) Phase II trial of murine (131)I-labeled antitenascin monoclonal antibody 81C6 administered into surgically created resection cavities of patients with newly diagnosed malignant gliomas. J Clin Oncol 20:1389-1397.

Rebischung C, Hoffmann D, Stefani L, Desruet MD, Wang K, Adelstein SJ, Artignan X, Vincent F, Gauchez AS, Zhang H, Fagret D, Vuillez J, Kassis AI, Balosso J (2008) First human treatment of resistant neoplastic meningitis by intrathecal administration of MTX plus (125)IUdR. Int J Radiat Biol 84:1123-1129.

Roberts DJ, Jr. (1979) ^{32}P-sodium phosphate treatment of metastatic malignant disease. Clin Nucl Med 4:92-93.

Roeda D, Kuhnast B, Hammadi A, Dolle F (2007) The Service Hospitalier Frederic Joliot - Contributions to PET chemistry over the years. J Labelled Comp Radiopharm 50:848-866.

Rogers IS, Nasir K, Figueroa AL, Cury RC, Hoffmann U, Vermylen DA, Brady TJ, Tawakol A (2010) Feasibility of FDG imaging of the coronary arteries: comparison between acute coronary syndrome and stable angina. JACC Cardiovasc Imaging 3:388-397.

Rosenblat TL, McDevitt MR, Mulford DA, Pandit-Taskar N, Divgi CR, Panageas KS, Heaney ML, Chanel S, Morgenstern A, Sgouros G, Larson SM, Scheinberg DA, Jurcic JG (2010) Sequential cytarabine and alpha-particle immunotherapy with bismuth-213-lintuzumab (HuM195) for acute myeloid leukemia. Clin Cancer Res 16:5303-5311.

Rudd JH, Warburton EA, Fryer TD, Jones HA, Clark JC, Antoun N, Johnstrom P, Davenport AP, Kirkpatrick PJ, Arch BN, Pickard JD, Weissberg PL (2002) Imaging atherosclerotic plaque inflammation with [^{18}F]-fluorodeoxyglucose positron emission tomography. Circulation 105:2708-2711.

Rufini V, Treglia G, Perotti G, Giordano A (2013) The evolution in the use of MIBG scintigraphy in pheochromocytomas and paragangliomas. Hormones 12:58-68.

Ruggiero A, Villa CH, Holland JP, Sprinkle SR, May C, Lewis JS, Scheinberg DA, McDevitt MR (2010) Imaging and treating tumor vasculature with targeted radiolabeled carbon nanotubes. Int J Nanomed 5:783-802.

Rutherford E (1919) Atomic projectiles and their collisions with light atoms. Science 50:467-473.

Schoffelen R, Boerman OC, Goldenberg DM, Sharkey RM, van Herpen CM, Franssen GM, McBride WJ, Chang CH, Rossi EA, van der Graaf WT, Oyen WJ (2013) Development of an imaging-guided CEA-pretargeted radionuclide treatment of advanced colorectal cancer: first clinical results. Br J Cancer 109:934-942.

Sharkey RM, Karacay H, Cardillo TM, Chang CH, McBride WJ, Rossi EA, Horak ID, Goldenberg DM (2005) Improving the delivery of radionuclides for imaging and therapy of cancer using pretargeting methods. Clin Cancer Res 11:7109s-7121s.

Shimizu T (1921) A reciprocating expansion apparatus for detecting ionizing rays. Proc R Soc Lond A 99:425-431.

Shirley M, McCormack PL (2014) Radium-223 dichloride: a review of its use in patients with castration-resistant prostate cancer with symptomatic bone metastases. Drugs 74:579-586.

Smit BS, Slabbert JP, Reinecke SA, Bohm L (2001) Comparison of cell inactivation by Auger electrons using the two reagents 4-[^{123}I]iodoantipyrine and [^{123}I]NaI. Radiat Environ Biophys 40:47-52.

Sofou S, Kappel BJ, Jaggi JS, McDevitt MR, Scheinberg DA, Sgouros G (2007) Enhanced retention of the alpha-particle-emitting daughters of Actinium-225 by liposome carriers. Bioconjug Chem 18:2061-2067.

Sogbein OO, Pelletier-Galarneau M, Schindler TH, Wei L, Wells RG, Ruddy TD (2014) New SPECT and PET radiopharmaceuticals for imaging cardiovascular disease. Biomed Res Int 2014:942960.

Strickland DK, Vaidyanathan G, Zalutsky MR (1994) Cytotoxicity of alpha-particle-emitting m-[^{211}At]astatobenzylguanidine on human neuroblastoma cells. Cancer Res 54:5414-5419.

Syed R, Bomanji J, Nagabhushan N, Kayani I, Groves A, Waddington W, Cassoni A, Ell PJ (2006) ^{186}Re-HEDP in the treatment of patients with inoperable osteosarcoma. J Nucl Med 47:1927-1935.

Tennvall J, Brans B (2007) EANM procedure guideline for ^{32}P phosphate treatment of myeloproliferative diseases. Eur J Nucl Med Mol Imaging 34:1324-1327.

Thomson JJ (1897) Cathode rays. Phyl Mag 44:293-316.

Ting G, Chang CH, Wang HE (2009) Cancer nanotargeted radiopharmaceuticals for tumor imaging and therapy. Anticancer Res 29:4107-4118.

Torchilin V (2011) Tumor delivery of macromolecular drugs based on the EPR effect. Adv Drug Deliv Rev 63:131-135.

Treglia G, Giovannini E, Di Franco D, Calcagni ML, Rufini V, Picchio M, Giordano A (2012) The role of positron emission tomography using carbon-11 and fluorine-18 choline in tumors other than prostate cancer: a systematic review. Ann Nucl Med 26:451-461.

Ullrich R, Backes H, Li H, Kracht L, Miletic H, Kesper K, Neumaier B, Heiss WD, Wienhard K, Jacobs AH (2008) Glioma proliferation as assessed by 3'-fluoro-3'-deoxy-L-thymidine positron emission tomography in patients with newly diagnosed high-grade glioma. Clin Cancer Res 14:2049-2055.

van Duijnhoven SM, Robillard MS, Nicolay K, Grull H (2011) Tumor targeting of MMP-2/9 activatable cell-penetrating imaging probes is caused by tumor-independent activation. J Nucl Med 52:279-286.

Verberne HJ, Brewster LM, Somsen GA, Eck-Smit BL (2008) Prognostic value of myocardial ^{123}I-metaiodobenzylguanidine (MIBG) parameters in patients with heart failure: a systematic review. Eur Heart J 29:1147-1159.

Volker JF, Hodge HC, Wilson HJ, van Voorhis SN (1940) The adsorption of fluorides by enamel, dentin, bone, and hydroxyapatite as shown by the radioactive isotope. J Biol Chem 134:543-548.

Volkert WA, Deutsch EA (1993) Bone seeking radiopharmaceuticals in cancer therapy. In Abrams MJ, Murrer B, eds., Advances in Metals in Medicine. JAI Press, Connecticut, 115-153.

Volkert WA, Goeckeler WF, Ehrhardt GJ, Ketring AR (1991) Therapeutic radionuclides: production and decay property considerations. J Nucl Med 32:174-185.

Volkert WA, Hoffman TJ (1999) Therapeutic radiopharmaceuticals. Chem Rev 99:2269-2292.

Wackers FJ, Berman DS, Maddahi J, Watson DD, Beller GA, Strauss HW, Boucher CA, Picard M, Holman BL, Fridrich R (1989) Technetium-99m hexakis 2-methoxyisobutyl isonitrile: human biodistribution, dosimetry, safety, and preliminary comparison to thallium-201 for myocardial perfusion imaging. J Nucl Med 30:301-311.

Werner ME, Karve S, Sukumar R, Cummings ND, Copp JA, Chen RC, Zhang T, Wang AZ (2011) Folate-targeted nanoparticle delivery of chemo- and radiotherapeutics for the treatment of ovarian cancer peritoneal metastasis. Biomaterials 32:8548-8554.

Wilbur DS, Hamlin DK, Meyer DL, Mallett RW, Quinn J, Vessella RL, Press OW (2002) Streptavidin in antibody pretargeting. 3. Comparison of biotin binding and tissue localization of 1,2-cyclohexanedione and succinic anhydride modified recombinant streptavidin. Bioconjug Chem 13:611-620.

Wilson JS, Gains JE, Moroz V, Wheatley K, Gaze MN (2014) A systematic review of ^{131}I-meta iodobenzylguanidine molecular radiotherapy for neuroblastoma. Eur J Cancer 50:801-815.

Witzig TE (2013) Moving radioimmunotherapy forward for follicular lymphoma. J Clin Oncol 20:294-296.

Witzig TE, Fishkin P, Gordon LI, Gregory SA, Jacobs S, Macklis R, McLaughlin P, Press O, Zelenetz AD (2011) Treatment recommendations for radioimmunotherapy in follicular lymphoma: a consensus conference report. Leuk

Lymphoma 52:1188-1199.
World Nuclear Association (2010) Radioisotopes in medicine. Available: http://www.world-nuclear.org.
Wuest F (2007) Fluorine-18 labeling of small molecules: the use of ^{18}F-labeled aryl fluorides derived from no-carrier-added [^{18}F]fluoride as labeling precursors. In Schubiger PA, Lehmann L, Friebe M, eds., PET chemistry. Springer, Berlin, 51-78.
Xing Y, Zhao J, Conti PS, Chen K (2014) Radiolabeled nanoparticles for multimodality tumor imaging. Theranostics 4:290-306.
Zalutsky MR, Bigner DD (1996) Radioimmunotherapy with alpha-particle emitting radioimmunoconjugates. Acta Oncol 35:373-379.
Zalutsky MR, Reardon DA, Akabani G, Coleman RE, Friedman AH, Friedman HS, McLendon RE, Wong TZ, Bigner DD (2008) Clinical experience with alpha-particle emitting ^{211}At: treatment of recurrent brain tumor patients with ^{211}At-labeled chimeric antitenascin monoclonal antibody 81C6. J Nucl Med 49:30-38.
Zalutsky MR, Reardon DA, Pozzi OR, Vaidyanathan G, Bigner DD (2007) Targeted alpha-particle radiotherapy with ^{211}At-labeled monoclonal antibodies. Nucl Med Biol 34:779-785.
Zubillaga MB, Boccio JR, Nicolini JO, Ughetti R, Lanari E, Caro RA (1996) Use of colloids of chromic [^{32}P] phosphate in treatment of solid tumors. Nucl Med Biol 23:907-910.
Zustovich F, Fabiani F (2014) Therapeutic opportunities for castration-resistant prostate cancer patients with bone metastases. Crit Rev Oncol Hematol 91:197-209.

Appendix. Characteristics of medical radionuclides.

Nuclide	$t_{1/2}$	Decay	Production	Application
C-11	20.4 m	β^+ 0.96 MeV	cyclotron	In PET for studying brain physiology, pathology, for localising epileptic focus, and in dementia, psychiatry and neuropharmacology studies; also in cardiology; [^{18}F]fluorodeoxyglucose (FDG) in cancer detection and in monitoring the progress of treatment, [^{18}F]fluorothymidine (FLT), [^{18}F]fluoromisonidazole (FMISO), [^{18}F]fluorocholine (FCH)
N-13	10.0 m	β^+ 1.19 MeV	cyclotron	
O-15	2.0 m	β^+ 1.72 MeV	cyclotron	
F-18	109.7 m	β^+ 0.64 MeV	cyclotron	
Na-24	15 h	β^- 1.39 MeV γ 1.37, 2.75, 3.87 MeV	reactor	electrolyte studies within the body
P-32	14.3 d	β^- 1.71 MeV	reactor	treatment of polycythemia vera (excess red blood cells) and essential thrombocyhtaemia, to treat bone pain from metastatic diseases
K-42	12.4 h	β^- 3.56, 1.97 MeV γ 1.52, 0.31 MeV	reactor	to study potassium distribution in body fluids; detection of brain tumors
Cr-51	27.7 d	EC (320 keV γ)	cyclotron	red blood cell labelling for measuring their volume, survival and splenic sequestration; quantification of gastro-intestinal protein loss
Fe-59	44.5 d	β^- 1.57, 0.475, 0.273 MeV γ 1.29, 1.09, 0.19, 0.14 MeV	reactor	to study iron metabolism in the spleen, diagnosis of aplastic anemia, iron deficiency anemia, leukemia, and polycythemia
Co-57	271.6 d	EC (136, 122, 14 keV γ)	cyclotron	diagnosis of pernicious anemia and defects of intestinal absorption
Co-60	5.27 y	β^- 315 keV γ 1.33, 1.17 MeV	reactor	sterilization
Cu-64	12.7 h	EC (1.64 MeV γ) β^- 0.57 MeV β^+ 0.66 MeV	cyclotron	to study genetic diseases affecting copper metabolism, e.g. Wilson's and Menke's diseases, and for PET imaging of tumors ([^{64}Cu]ATSM), and targeted therapy (Asabella et al. 2014)
Cu-67	62.0 h	β^- 577, 484, 395 keV γ 185 and 92 keV	cyclotron	targeted therapy (Asabella et al. 2014)
Ga-67	78.3 h	EC (388, 296, 184, 93 keV γ)	cyclotron	SPECT tumor imaging (gallium citrate) for Hodgkin's disease, lymphomas and bronchogenic carcinoma; localisation of acute inflammatory lesions
Ga-68	68.3 m	β^+ 1.90 MeV EC (1.87, 1.24, 1.08, 0.80 MeV γ)	generator (from Ge-68)	tumor imaging, especially leukocyte-derived malignancies by PET
Se-75	119 d	EC (401, 280, 265, 136, 121, 97, 66 keV γ; 14 keV e^-; As K X-ray)	reactor	investigation of the enterohepatic circulation of bile salts, diagnostic liver scanning (Boyd et al. 1981)
Kr-81m	13.1 s	IT (191 keV γ)	generator (from Rb-81)	imaging of pulmonary ventilation, early diagnosis of lung diseases and function
Rb-82	1.26 m	β^+ 3.18 MeV	generator (from Sr-82)	myocardial perfusion PET imaging
Sr-89	50.5 d	β^- 1.49 MeV	reactor	palliative in prostate and bone cancer
Y-90	64.0 h	β^- 2.28 MeV	reactor	cancer brachytherapy, liver cancer therapy, for relieving the pain of arthritis in larger synovial joints
Tc-99m	6 h	IT (140 keV γ)	generator (from Mo-99)	the most common diagnostic radioisotope for imaging the skeleton, heart muscle, brain, thyroid, lungs, liver, spleen, kidney, gall bladder, bone marrow, salivary and lacrimal glands, heart blood pool
Pd-103	17 d	EC (498, 362, 297 keV γ; 43 keV e^-) Rh K X-rays	reactor	brachytherapy with sealed implants for early stage prostate cancer
In-111	2.83 d	EC (247, 173 keV γ)	cyclotron	tumor imaging, platelet labelling, localization of inflammation, colon transfer studies
I-123	13.0 h	EC (159 keV γ)	cyclotron	γ emitter without the beta radiation of I-131, thyroid gland imaging, treatment of thyroid metastases, pheochromocytoma
I-124	4.15 d	EC (1.69, 0.73, 0.61 MeV γ) β^+ 2.13, 1.53, 0.8 MeV	cyclotron	PET imaging (Koehler et al. 2010)
I-125	60.2 d	EC (35 keV γ) 18 keV e^-	reactor	prostate and brain cancer brachytherapy, determination of glomerular filtration rate, diagnosis of deep vein thrombosis in the leg; widely used in radioimmuno-assays to measure hormone levels
I-131	8.04 d	β^- 806, 607, 336 keV, 10 keV e^- γ 637, 364, 284, 80 keV 32 keV Xe K X-ray	reactor	blood volume/plasma volume determination; thyroid imaging, beta therapy of thyroid cancer; diagnosis of abnormal liver function, renal blood flow and urinary tract obstruction; treatment of refractory low-grade non-Hodgkin's lymphoma

Nuclide	$t_{1/2}$	Decay	Production	Application
Xe-133	5.2 d	β^- 346 keV γ 81 keV, 36 keV e^- Cs K and L X-ray	reactor	investigation of pulmonary function, lung ventilation imaging (Jones et al. 1978)
Cs-137	30.1 y	β^- 1.18, 0.51 MeV γ 662 keV	reactor	low-intensity sterilization of blood
Sm-153	46.8 h	β^- 810, 710, 640 keV γ 103, 70 keV 45 keV e^- Eu K and L X-rays	reactor	palliative in osteoblastic metastatic bone lesions, treatment of prostate and breast cancer
Dy-165	2.3 h	β^- 1.31, 1.22 MeV γ 716, 633, 361, 95 keV 52 keV Ho K X-ray	reactor	synovectomy treatment of arthritis
Ho-166	2.8 h	β^- 1.85, 1.77 MeV 81 keV γ		diagnosis and treatment of liver tumors
Er-169	9.4 d	β^- 340, 332 keV 8 keV γ	reactor	relieving arthritis pain in synovial joints
Yb-169	32.0 d	EC (308, 198, 177, 131, 110, 63 keV γ; 112 keV e^-) Tm K and L X-rays		cerebrospinal fluid studies in the brain
Lu-177	6.71 d	β^- 497, 384, 249, 175 keV γ 208, 113 keV 15 keV e^- Hf K and L X-rays	reactor	bone imaging, treatment of arthritis and neuroendocrine tumors (Kam et al. 2012)
Re-186	90.6 h	β^- 1.07, 0.93 MeV γ 137, 122 keV 14 keV e^- W and Os K X-rays	reactor	palliative in bone metastases, bone scintigraphy, radiosynovectomy (Ogawa et al. 2007)
Re-188	17 h	β^- 2.12, 1.97 MeV γ 932, 633, 478, 155 keV 16 keV e^- Os K and L X-rays	generator (from W-188)	treatment of metastatic bone cancer, non-resectable liver cancer, non-melanoma skin cancer, treatment of arthritis; inhibition of arterial restenosis following balloon angioplasty; endovascular radiation therapy
Ir-192	74.2 d	β^- 672, 536, 240 keV) EC (612, 604, 589, 468, 317, 308, 296 keV γ; 45 keV e^-)	reactor	internal source for cancer treatment
Tl-201	74 h	EC (135, 167 keV γ; 48 keV e^-)	cyclotron	diagnosis of coronary artery disease, heart muscle death, for location of low-grade lymphomas; the most common substitute for Tc-99 in cardiac-stress tests
Pb-212	10.6 h	β^- 568, 331 keV γ 300, 238 keV 74 keV e^- Bi K and L X-rays	generator (from Ra-224)	targeted alpha immunotherapy (in vivo generates the emitters Bi-212 and Po-212) for melanoma, breast and ovarian cancer (Milenic et al. 2005)
Bi-213	47 m	α 5.8, 5.5 MeV β^- (8.4 MeV α from Po-213)	generator (from Ac-225)	alpha immunotherapy, cancer therapy